5-2022

Structural Analysis of [Ni(dippe)] Fragment Using Computational Methods

Jennifer L. Sanchez
The University of Texas Rio Grande Valley

STRUCTURAL ANALYSIS OF [NI(DIPPE)] FRAGMENT USING COMPUTATIONAL METHODS

A Thesis

by

JENNIFER L. SANCHEZ

Submitted in Partial Fulfillment of the

Requirements for the Degree of

MASTER OF SCIENCE

Major Subject: Chemistry

The University of Texas Rio Grande Valley

May 2022

STRUCTURAL ANALYSIS OF [NI(DIPPE)] FRAGMENT USING COMPUTATIONAL METHODS

A Thesis
by
JENNIFER L. SANCHEZ

COMMITTEE MEMBERS

Dr. Tülay A. Ateşin
Chair of Committee

Dr. William D. Jones
Committee Member

Dr. Manar Shoshani
Committee Member

Dr. Evangelia Kotsikorou
Committee Member

May 2022

ABSTRACT

Sanchez, Jennifer L., Structural Analysis of [Ni(dippe)] Fragment using Computational Methods. Master of Science (MS), May, 2022, 58pp., 8 tables, 25 figures, references, 52 titles.

The structural analysis of the Nickel (Bisdiisopropylphospino)ethane, also known as $[Ni(dippe)H]_2$, has been heavily studied in our group in collaboration with William D. Jones's group. A computational analysis of the [Ni(dippe)] fragment was performed to determine the structural relationship between the nickel center and its phosphine ligand, due to phosphines having both electronic and steric properties. The reactivity of the Nickel will be most dependent on the dippe ligand. A conformational search generated 244 conformers after a thorough minimization using Molecular Mechanic (MM) calculations where a thorough minimization was performed and then re-minimized using a SEED command until unique conformers remained. Quantum Mechanical (QM) calculations were then performed using DFT to optimize the 244 conformers and then duplicates were further removed, where 177 unique conformers remained. The lowest five energy conformers below 1.0 kcal/mol were studied heavily to better understand the 3D structure of the [Ni(dippe)] fragment. The conformers associated with the five-membered chelate rings (λ/∂) and the isopropyl groups (anti/gauche) were systematically analyzed. The Boltzmann distribution of the conformers generated will be presented. This study can be applied in the growing field of Ni-catalyzed reactions with bidentate phosphines.

DEDICATION

First, I would like to dedicate this thesis to my loving parents, Veronica and Javier Sanchez. Without their support, both financially and emotionally, I would not have been able to focus so heavily on my studies as I did. Secondly, I would also like to dedicate this work to my siblings Stephanie and Nancy Sanchez, for providing laughter and peace in a time of great stress in my life. Without their sisterly love then this journey would have been solemn. Finally, I would like to dedicate this work to Melesio Ruvalcaba, the love of my life, who has stuck by my side since the beginning of my journey as a new student in Chemistry. Through his love, comfort, and reliability, I was able to overcome many difficulties and push forward in my journey as a Chemist and Master student.

ACKNOWLEDGMENTS

I would like to acknowledge my advisor, my mentor, and thesis committee chair, Dr. Tülay Ateşin, for always providing great guidance and accepting me as her research student since an Undergraduate. She placed her confidence in me and believed I would always reach my goal, without her then I'm not confident that I would have accomplished as much as I did. I would also like to thank Dr. Abdurrahman Ateşin, I would not have known as much as I do about computer software without him. Both being great mentors to me and have also allowed me to become more confident in myself and to break a little away from my old shy-self. Additionally, a big thank you to my committee members Dr. William Jones, Dr. Manar Shoshani, and Dr. Evangelia Kotsikorou for providing additional guidance. It was a great honor to work with Dr. Jones and this important opportunity allowed me to grow as a chemist and become more confident in my work as an organometallic chemist. Learning under Dr. Manar's guidance has allowed me to grow as a material chemist, he has given me great advice on how to study crystals computationally. Dr. Kotsikorou has always been willing to give me her helpful input on my computational calculations, which my work has benefitted greatly for. Without my committee members, I would not be the well-rounded chemistry I am, disciplined in multiple areas in chemistry. Finally, I would like to thank the University of Texas Rio Grande Valley and the Chemistry Department for providing me with a great experience and funding as an undergraduate and graduate student.

TABLE OF CONTENTS

Page

LIST OF TABLES

Page

LIST OF FIGURES

Page

CHAPTER I

INTRODUCTION

Group 10 Metals: Nickel, Palladium, and Platinum

Nickel, palladium, and platinum are important transition metals that are heavily studied in Organometallic Chemistry. These three metals make up the Group 10 column, located in the center, d-block, portion of the periodic table. Both palladium and platinum are considered to be part of the "precious metals" group, which also include gold and silver. They are very expensive due to their scarcity but are great metals to use in organometallic complexes as catalysts because of their great attributes, one being stability, unlike their close neighbor nickel.1 Nickel is abundant in nature, making it one of the most common metals found on earth. Typically, its used to make stainless steel, alloys, catalysts, superalloys, and rechargeable batteries, as reported by the United States Geological Survey.2 Despite these positive attributes, nickel is reactively and electronically different compared to palladium and platinum in a disadvantageous way. Due to its difficulty to work with and unpredictable reactivity, nickel was dubbed the "spirited horse" by Nobel prize laureate Paul Sabatier in 1922.3 Organometallic chemists have made significant strides to "tame" nickel, allowing it to step into the spot-light as a strong contender as a catalyst.

To truly understand nickel's faults, it important to compare and contrast all of the Group 10 metal's reactivity and characteristics. First, regarding electronegativity (EN), Pauling defined EN in 1932 as the tendency of an atom in a molecule to attract electrons to itself, such as the atomic number.4 A good example of this, is the Lanthanoid contraction, where the 3rd row of the

transition metals have a slightly higher EN values than the 2nd row, as shown by Dongfeng Xue.5 It was also noted that these larger EN values are due to longer relativistic effects. Dongfeng Xue also shows how the stability of a divalent metal (M^{2+}) ion corresponding to complexes increases by: $Mn^{2+}<Fe^{2+}<Co^{2+}<Ni^{2+}<Cu^{2+}>Zn^{2+}$, which is in agreement with Irving-William order for the stability of a metal complex.[5,6] This information is important for Organometallic chemists in determining how metals interact with their paired ligands. These characteristics intertwine, and can all affect a metals activity, and when a ligand is introduced then the reactivity also becomes affected.

Nickel has also been shown to undergo different organometallic reactions when used in C–C bond activation. Both palladium and platinum are fairly stable metals compared to nickel and have been shown to undergo reductive elimination more readily, while nickel undergoes facile oxidative addition because of its oxophilic nature.[1,7] It is also notable how nickel also goes through β-migratory insertion while palladium and platinum undergo facile β-hydride elimintation.7 These reaction steps will be further explored in more detail the *Ni C–CN Bond Activation* section. Another characteristic that differs between these 3 metals are their Bond Dissociation Energies (BDE), when bonded to carbon. Within the Group 10 metals, it was noted that the M–C bond strength changes in the order of Ni–C < Pd–C < Pt–C, reactivity also decreases from Ni to Pd, and then to Pt, while the homolytic M–C bond cleavage trend follow: Ni–C > Pd–C > Pt–C, as noted by Valentine Ananikov.3 Although nickel is very different compared to palladium and platinum, it has been used and adapted to various applications in chemistry.

CHAPTER II. BACKGROUND

Ligand Choice: (Bisdiisopropylphosphino)ethane and (Bisdimethylphosphino)ethane

Choosing a ligand plays a big role in how it will sterically and electronically affect the overall organometallic catalyst. Phosphine ligands are widely known to be great π-acceptors, electron-rich, and have been found to enhance the rate of both oxidative addition and reductive elimination.8 Tolman studied the change in molecular properties which derived from a change occurring with part of a molecule, both steric and electronic. Where he showed that an increase in size of the substituent on the phosphor atoms will favor oxidative addition, isomers which are less crowded, and how various phosphor ligands competed for coordination on Ni(0) using the ligand cone angle steric parameter, θ, arguing that steric effect is just as important as electronic effect.[9] While a study done by Van Leeuwan, shows how the electronic nature is the main driving force affecting palladium diphosphine complex reductive elimination energy barriers rather than its steric effects. It is important to study both the steric effect that the phosphine ligand has on nickel and how it might later affect the square planar geometry. The bite angle of phosphine ligands are noted to affect the stability of the square planar nature of Pd(II) complexes. As well as Ni(0) complexes, where a 90˚ angle stabilizes a Ni square planar system but an increase of the bite angle could lead to an increased stabilization of Ni tetrahedral system and a destabilization of the square planar system.[10,11,12,13] Recently, Jones et. al. showed that different Lewis acids have been shown to enhance the reaction rate by using less than one

equivalent, while using one equivalent or more inhibit the reaction.[14] It was also found that Lewis acids can also increase the rate of reductive elimination in Pd phosphine complexes.[14,15] Among the most commonly used phosphine ligands, there is a choice to make between monophosphine ligands and diphosphine, or bidentate, ligands.

It is known that a bulkier ligand will create a sterically crowded system which can affect bending, repulsion, bite angle, and flexibility. Bulky ligands can be shown to have both steric repulsion and steric attraction. Steric attraction can occur from more planar bulky ligands and can bend their large surfaces toward each other, causing a favored stabilization and enhancing nonlinearity or bite-angle flexibility. Wolters et. al. reported that $Pd(PPh_3)_2$ showed the lowest energy barrier compared to the smallest tested catalyst complex, $Pd(PH_3)_2$, confirming the effect on oxidative addition barriers by the steric nature of the bite-angle. A smaller bite angle is known to lead to a lower reaction barrier for oxidative addition because of less steric repulsion between the ligand and substrate.[16] Monophosphine ligands also have a tendency to cause unwanted off-pathway reactions which then leads to lower yields and selectivity.[17] Bidentate phosphines were shown to be good for oxidative addition reactions for C–P ligands.[18] Therefore, for our system we will be focusing on using bidentate phosphine ligands.

The most commonly used diphosphine ligands are shown in **Figure 1**. It is important to choose the right bidentate phosphine ligand because they each have their own effect on the reaction which can lead to different outcomes. For example, it was reported that the dppp ligand in $[Rh(nbd)dppp]PF_6$ supports an alkene insertion in the α C–C bond, while replacing the dppp ligand with dppb showed that a wider bite angle caused Rh to favor a four-membered ring which then promoted a decarbonylation pathway. Taking it further, replacing the dppp ligand with dppe then caused cleavage with the β C–C ligand which then undergoes β-hydride elimination and

reductive elimination.[19] The dmpe and dippe ligand are often employed in the Jones group.[20,21] For DFT calculations, the dmpe ligand is switched out for dippe due to its simplicity and lowers the computation time. Both Ni(dmpe) and Ni(dippe) complexes are observed in acetonitrile and benzonitrile. The importance of Ni(dippe) complexes is great and can be applied to various fields within the world of chemistry. Studying the [Ni(dippe)] fragment can help with a deeper understanding of the steric effects that the dippe ligand has on the Ni metal center.

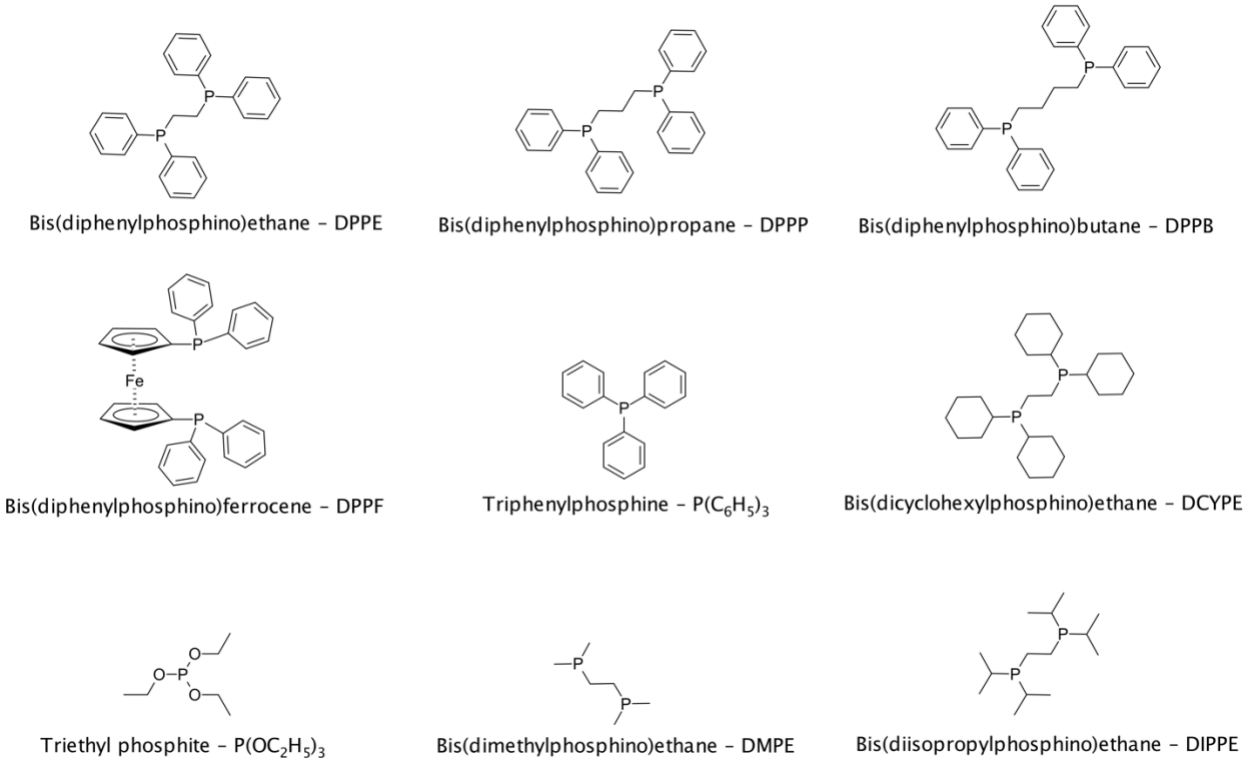

Figure 1: Commonly used bidentate phosphine ligands with their abbreviations.

Reactions and Applications of [Ni(dippe)]

[Ni(dippe)] has been used an array of reactions and is applied in Environmental, Energy, Industrial, Materials, and Pharmaceutical chemistry. Garcia's group has focused on the cleavage of C–S bonds through hydrosulfurization which in turn can reduce the air pollution of noxious sulfur oxides. Their group have also carried out a Suzuki-Miyaura type reaction, highlighting the

process of desulfurization of dibenzothiophene and dibenzothiophene sulfones using [Ni(dippe)].[22] Where they achieved high conversions and produced a variety of poly-phenyl compounds and were also able to observe waters role in yielding *o*-terphenyls, as shown in **Figure 2**.

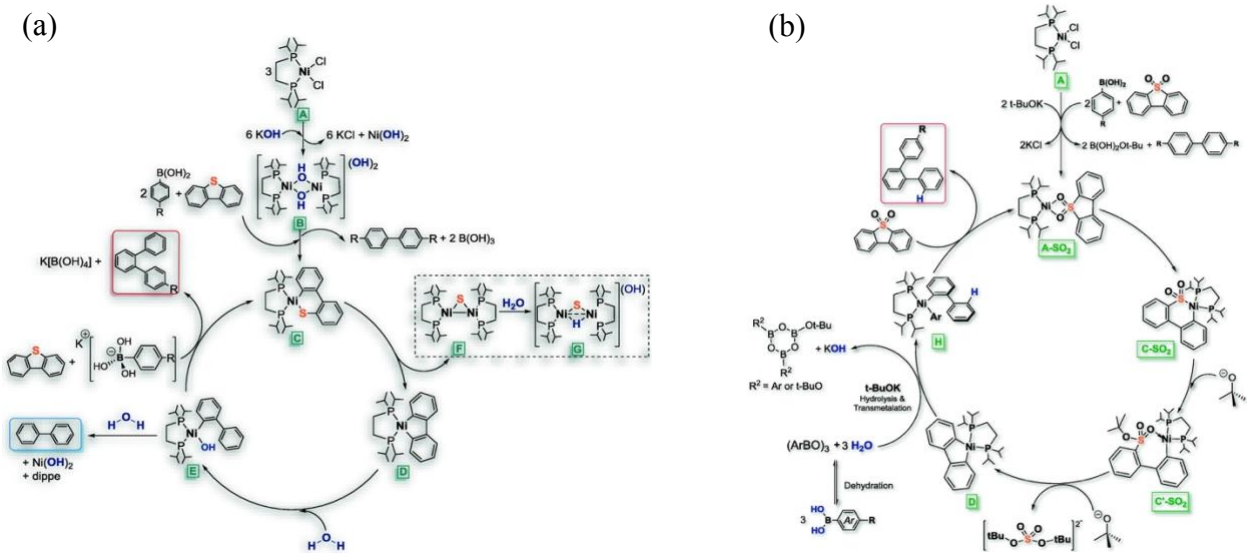

Figure 2: Proposed mechanism for (a) dibenzothiophene and (b) dibenzothiophene sulfone desulfurization, as reported by Garcia et. al.[22] with permission from Elsevier.

Other reactions [Ni(dippe)] has been used in, include electroreduction where it undergoes protonation to produce nickel hydride which then generates H_2 for hydrogen fuel.[23] In Energy Chemistry, it has been used to depolymerize lignin by cleaving the ether bonds to create bio fuel.[23] In Energy Chemistry, nickel catalysts are utilized to suppress methanation reactions in water-gas shift reactions.[24] [Ni(dippe)] is also utilized in trifluoromethylation of aryl halides.[25] A challenging study was undertaken for Ni-catalyzed nucleophilic trifluoromethylation of aryl halides, where DFT calculations showed that dppf and dcypf were good candidates to perform synthesis with but unfortunately failed to obtain Ar–CF_3 reductive elimination with Ni(II). Even

though it was a failure, some notable factors gathered from the experiment were that (1) Ni(II) complexes with fluoride trans to a non-electron-deficient aryl can exist and be stable and that complexes of the type [(PP)Ni(Ar)(CF_3)] can be prepared for diphosphines PP other than dippe, where PP is dppf and dcypf.

Finally, it is important to discuss more work done with [Ni(dippe)] within the Jones group, C–CN bond activation is the main focus due to the difficult task of cleaving the thermodynamically stable C–C bond, as shown in **Figure 3**.[27] Other reactions studied by the Jones group include Lewis acid assisted C–CN bond activation, DFT calculations regarding DuPont adiponitrile process (ADN), C–S, C–C, and C–H bond activation, and of course their scope also covers the group 10 transition metals: Pd, Pt, and Ni.[14,20] Recently, their group has experimentally proposed a mechanism in regard to [Ni(dippe)] C–CN bond activation in benzonitrile. Therefore, it is imperative to study how the dippe ligand sterically interacts with the Ni metal center. This computational study can be compared with the Jones group experimental findings and will also be used for further research in our own group, where a future comparison between [Ni(dippe)], [Pd(dippe)], and [Pt(dippe)] will be conducted as well.

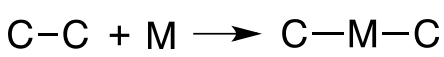

Figure 3: Metal insertion via bond cleavage of a thermodynamically stable C–C bond.

[Ni(dippe)] Crystal Structures

Jones group has published numerous papers on [Ni(dippe)] systems, but not all of the crystal structures have the same ligand conformation. It is important to check the lowest energy conformation [Ni(dippe)] adheres to, therefore making it to choose which structure will provide the best C–CN bond activation.

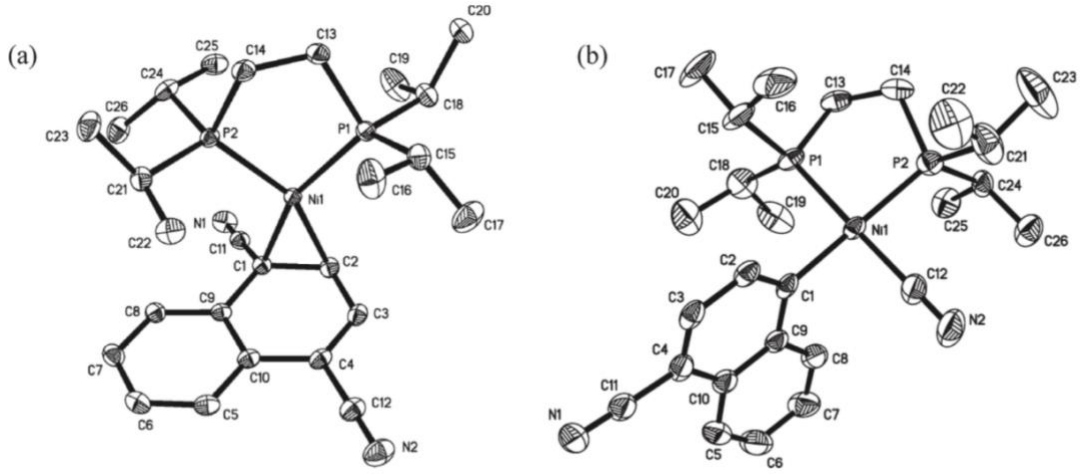

Figure 4: X-ray crystal structures of Ni(dippe)(1,2-η^2-1,4-dicyanonaphthalene) and Ni(dippe)(CN)(4-CN-naphthyl). Reprinted with permission from Jones et. al.[14] Copyright 2010 American Chemical Society.

Figure 4 shows the η^2 complex of Ni(dippe) with arene compounds in benzonitrile. It was shown that the $[Ni(dippe)H]_2$ complex prior to reacting it with dicyanobenzene was twisted at an 80˚ angle between the P(1)–Ni(1)–P(2) and P(1)A–Ni(1)A–P(2) planes. Through DFT calculations it was noted that the η^2 arene complex shown in **Figure 4 (a)** had a higher energy than the oxidative addition products shown in **Figure 4 (b)** but was not thermodynamically favored. There is also evidence that the C=C bond rotates around nickel. The bond lengths were listed, and the Ni(1)–C(1) and Ni(1)–C(2) bonds differ slightly and the angle between P(1)–Ni(1)–P(2) differ greatly, where for the η^2 product it is 92.09˚ and for the oxidative addition product it is 88.32˚.[14]

(a)

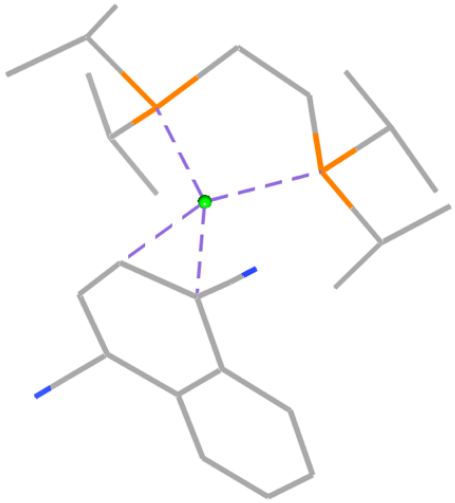

(b)

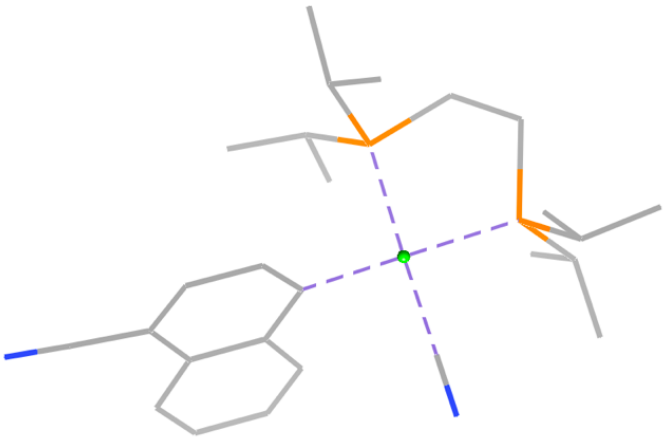

Figure 5: X-ray crystal structures of [Ni(dippe)] (a) η^2 coordinated and (b) Ni(dippe)(CN) with BPh_3 Lewis acid substrate in benzonitrile. The nickels are shown in green, the carbons in grey, the nitrogen in blue, the phosphor atoms in orange, and the hydrogens were hidden for clarity.

The crystal structures shown in **Figure 5** are also reacted in benzonitrile and a BPh_3 Lewis acid is used to assist the reaction. The angle between the C(1)–N(1)–B(1) greatly differed from each other, the η^2 complex had an angle of 143.4˚ while the angle for the oxidative addition

product was 175.94˚. There are many more crystal structures that are published within the Jones group and it is important to study how the ligand coordinates with the nickel metal center. To understand this the [Ni(dippe)] fragment has to be studied to see which conformation is the most stable and likely to occur.[14]

[Ni(dippe)] C–CN Bond Activation

C–CN bond activation has been a topic of interest since its emergence in the 1970s. It is widely known how the kinetic inaccessibility of the very stable C–C bond contributes to its lack of reactivity, an unfavorable situation for the less stable M–C bond formation. Although inconvenient, there have been strategies proposed and enacted to overcome these set-backs. These proposed pathways that are commonly seen with C–C bond cleavage with nickel catalysts are oxidative addition, β-carbon elimination, and retro allylation.

One of the most common pathways Ni-complexes can undergo is oxidative addition. Oxidative addition is the reverse reaction of reductive elimination, which can be seen in **Figure 6**. Transition metals such as platinum and palladium prefer the reductive elimination reaction while nickel being more oxophilic prefer oxidative addition.[1,8,28] Muetterties et. al. reported on the cleavage of C–C bonds in aryl nitriles, where it was noted that the ligand dissociation for four-coordinate Pt and Ni complexes happened rapidly at low concentrations through oxidative addition.[26]

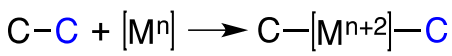

Figure 6: Insertion of a metal via oxidative addition.

While with a β-carbon elimination pathway, similar to a β-hydride elimination reaction, the metal alkyl is converted to a M–C bond through the strong driving force of the C=X bond formation, or the loss of the alkyl, where X=C, N, O.[29] This reaction can be seen in **Figure 7**, and has been observed to form thermodynamically favored five membered rhodacyclic complexes and benzaldehyde. For a strained cyclic substrate, the ring-strain release allows facile C–C bond cleavage and for acyclic substrates, a successful reaction occurs through an increased entropy generated from a stable byproduct formation.[30,31] Crabtree notes that this process occurs rapidly for d^2 and higher metals due to possible back-donation, which d^0 metals cannot do. The C–C bond is weakened enough to allow it to bond to the metal center, also providing stabilization to the alkene during the transition state.[23] More specifically, retro-allylation, shown in **Figure 7**, is a more specific case of β-carbon elimination where the C–C cleavage proceeds via a six-membered ring, generating regio- and sterodefined allyl-metal species.[32,33]

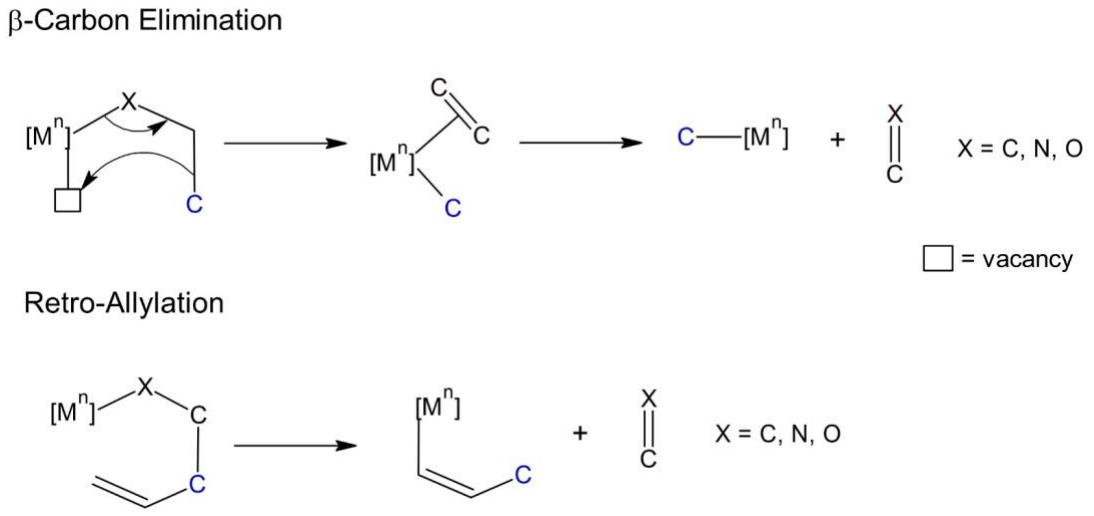

Figure 7: C–CN bond activation via β-carbon elimination, Retro-Allylation and β-hydride elimination.

Various pathways for C–CN bond activation were explored and tested on nickel complex systems besides the three mentioned previously, such as β-hydride shift, by silylrhodium(I) complexes, and the Dupont ADN process which can be seen in **Figure 8** used for the polymerization of nylon-6,6.[26] Where the nickel catalyst cleaves the C–CN bond of the 2-methyl-3-butenenitrile and converts it to 3-pentenenitrile and 4-pentenenitrile, where it undergoes hydrocyanation to produce ADN. This DuPont ADN process is a great early representation of C–CN bond activation, and in recent years the DuPont group has also taken an interest in the effect of Lewis acids on C–CN bond activation, similar to the Jones group.[30]

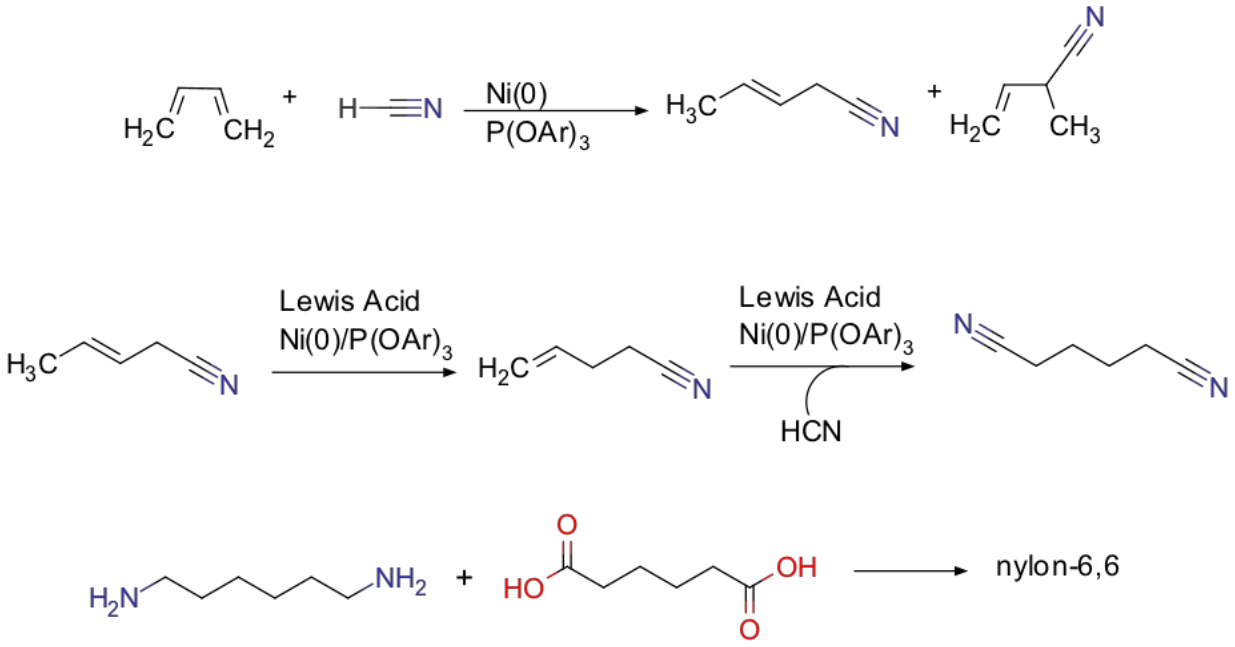

Figure 8: C–CN bond activation catalyzed with Ni(0)/P(OAr)$_3$ using Dupont ADN process for the polymerization production of nylon-6,6.

Generally, C–CN bond activation has two commonly accepted pathways. This can be seen in **Figure 9**, where the metal can insert itself through the use of Rh or Fe-SiR_3 catalyst or with the use of group 10 metals, Mo, and Rh.[29] In the Jones group, the activation of C–CN bond has been extensively studied for [Ni(dippe)] using both alkyl, allyl and aryl nitriles seen in **Figure 10**.

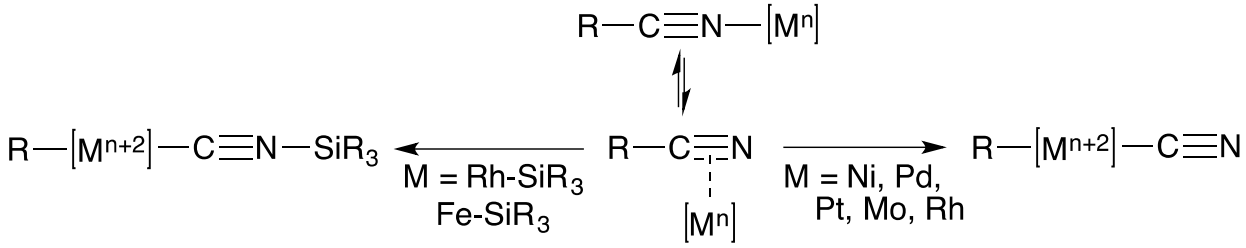

Figure 9: Two commonly accepted pathways for C–CN bond activation.

Achieving C–CN bond cleavage could be done through the use of $[Ni(dippe)H]_2$ as the source for the highly reactive [Ni(dippe)] fragment in acetonitrile. Where the η^2-nitrile complex facilitated the activation of C–CN and was reversible, it was also was shown to have better yields when slightly heated to 80˚C. For larger nitriles, it was shown that photochemical conditions were needed but C–CN bond activation was still achievable but as the size of the alkyl nitriles were increased the C–CN decreased drastically. The Jones group were also able to show the effect of Lewis Acids on this system, where it inhibits C–CN cleavage, leading to reductive elimination of RCN, which have been observed in palladium complexes as well.[34] Which is the opposite for Allyl nitriles where it was shown to accelerate and favor the C–CN bond activation while suppressing C–H activation.[35,36]

Alkyl Nitrile

(a)

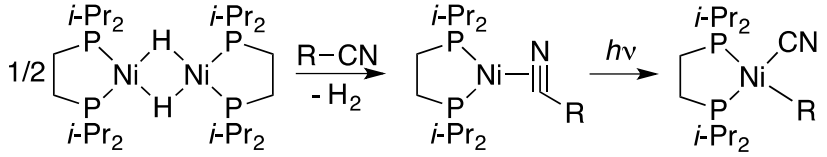

Allyl Nitriles

(b)

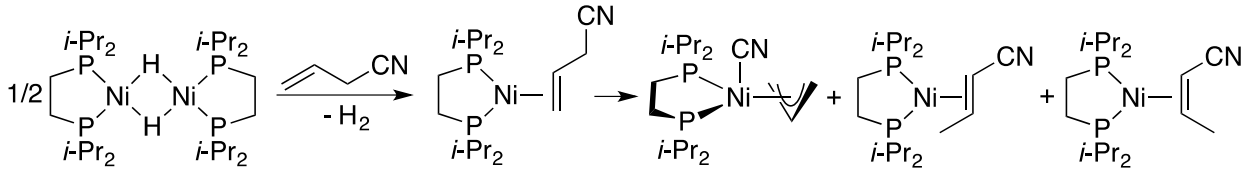

(c)

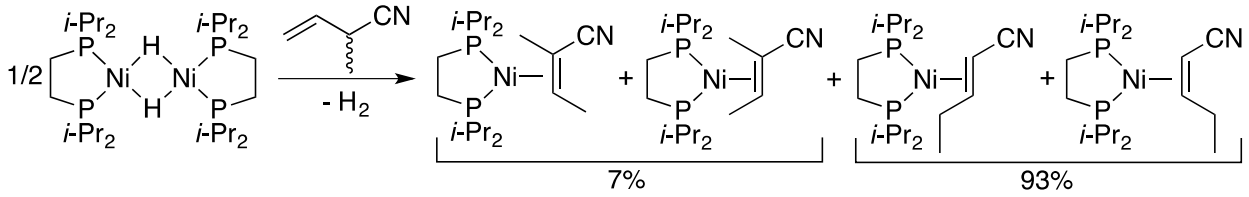

Aryl Nitrile

(d)

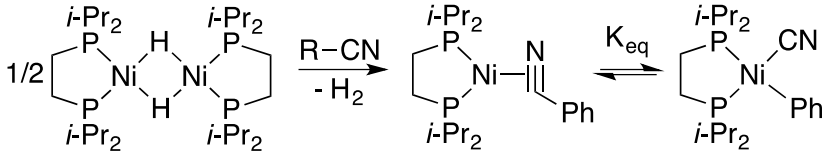

Figure 10: C–CN bond activation using $[Ni(dippe)H]_2$ using Alkyl, Allyl and Aryl nitriles.

Allyl nitriles are used in the DuPont ADN process, seen in **Figure 8**. It was shown that upon reacting $[Ni(dippe)H]_2$ with allyl cyanide, an η^2-olefin complex (dippe)Ni(allyl cyanide) was favored, where it is then isomerized rapidly. C–H and C–C bond activation are competitive with this η^2-olefin complex, where the obtained η^2 cis- and trans-crotonitrile complexes shown in **Figure 10 (b)** are thermodynamically favored compared to the square-pyramidal structure complex. The square-pyramidal (dippe)Ni(π-allyl)CN structure from the C–C bond activation converts to the cis and trans products indicating it is a reversible process and is kinetically competitive to C–H activation.[35] DFT calculations for the isomerization of 2-methyl-3-

butenenitrile in the DuPont ADN using $[Ni(dippe)H]_2$ was conducted which showed that the C–CN cleavage is kinetically favored to give olefin products over C–H cleavage, demonstrated in **Figure 10 (c)**.[37]

$[Ni(dippe)H]_2$ has been reacted in benzonitrile to produce a η^2-nitrile complex, (dippe)Ni(η^2-NCPh), shown in **Figure 10 (d)**. At room temperature in THF, this η^2 complex then converts to oxidative addition product (dippe)Ni(Ph)(CN) where it does not go to competition but instead remains in equilibrium, favoring the oxidative addition product.[38]

Lewis Acid Assisted Reactions with [Ni(dippe)], [Pd(dippe)], and [Pt(dippe)]

The Jones group has also been investigating the effect of Lewis Acids on C–CN bond activation using M(dippe) complexes, with a main focus on the group 10 metals. Experimental data has been collected for both nickel and palladium but not for platinum. In **Figure 11**, BF_3 and BPh_3 were two Lewis acids that had a profound effect on the reaction rate of $[Ni(dippe)H]_2$, when less than one equivalent is used then the reaction rate is 100 times greater but when more than one equivalent is used then the reaction is inhibited.[14]

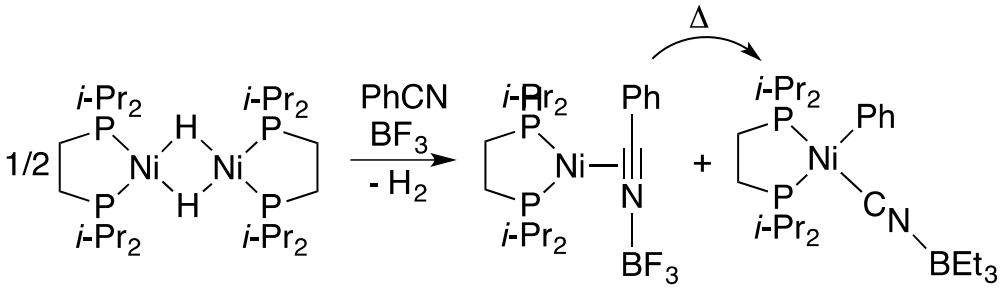

Figure 11: [Ni(dippe)] C–CN bond activation in Benzonitrile using BF_3.

While for palladium, it was shown that when reacted with BEt_3 or BPh_3 in acetonitrile, the Lewis acid attaches itself on the nitrogen by coordinating with the nitriles lone pair, forming the η^2 complex shown in **Figure 12.** This coordination has been shown to improve reaction rates, product selectivity, and through steric bulk or charge distribution on nitrogen or boron atom can extend catalyst lifetime. Under photochemical and thermal conditions the η^2 product can undergo C–CN bond cleavage to yield (dippe)Pd(Ph)(CN-BEt_3).[39]

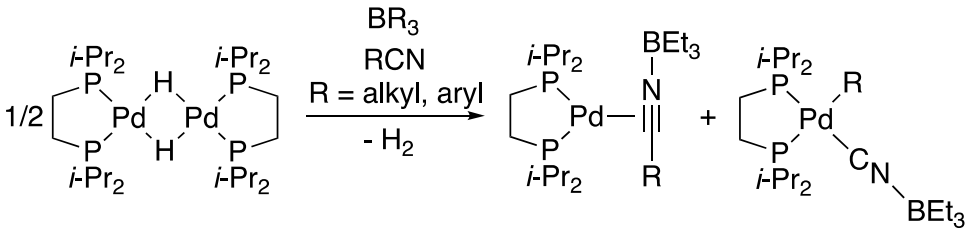

Figure 12: Lewis Acid Assisted C–CN bond activation with [Pd(dippe)] in acetonitrile and benzonitrile.

The last reaction that will be discussed is the $[Pt(dippe)H]_2$ in benzonitrile. Platinum has been shown to follow both C–C and C–H activation pathways, where PtL_2 fragments preferred oxidative addition by C–H bond cleavage. **Figure 1**3 shows the reaction of $[Pt(dippe)H]_2$ in PhCN, where three of the products were with C–H activation, which is kinetically favored, and one product (the second product) was from C–CN bond activation. A pathway using Lewis acids has not been observed with platinum and will be researched in the near future.[40]

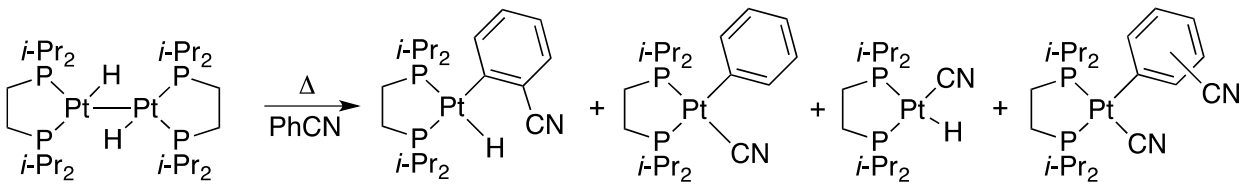

Figure 13: [Pt(dippe)] C–CN bond activation in benzonitrile.

CHAPTER III

METHODOLOGY

Computational Methods

A thorough conformational search for the low-energy conformers of [Ni(dippe)] fragment was performed by generating all the possible conformers by using MM methods implemented in Schrödinger MacroModel 2020-2.[41] After the energy minimization of the conformers with MM methods, the geometry optimization was conducted using QM methods in Gaussian 16 suite of program.

Conformational Search and Minimizations using MM Methods

The starting geometry of [Ni(dippe)] fragment was obtained from an available X-ray single crystal structure of a Ni complex containing the [Ni(dippe)] fragment and removing the rest of the molecule. The numbering of the atoms is displayed in **Figure 14**. The torsional angles C(2)-Pd(1)-P(18)-N(11) and C(4)-Pd(1)-N(5)-C(10) were fixed to preserve the square-planar coordination environment around the Pd(II) metal center. MM calculations were performed using Schrodinger Macromodel 2020-2.[41] A thorough conformational search was performed with a Mixed torsional/Low-mode sampling method[42] and OPLS3e forcefield[43]. The dielectric (ε) constant was set at 2.40 for toluene.[44]

Two independent conformational searches were conducted.

Starting from the X-ray single crystal structure of the [Ni(dippe)] fragment, the first set of conformers were generated. The Truncated Newton Conjugate Gradient (TNCG) minimization

method[45] was used for the geometry optimizations. The first minimization was done with a maximum iteration of 2500 steps and a convergence threshold of 0.05 kcal/mol. This minimization step was repeated until the number of conformers stayed the same. The maximum iteration was maximized to 9,999,999 steps and the convergence threshold was lowered to 0.001 kcal/mol gradually when the minimization steps hit a new plateau. Using the SEED command, we conducted another conformational search. The combined conformers were minimized again the same procedure. With each minimization the convergence threshold was gradually lowered from 0.0500 kcal/mol to 0.0002 kcal/mol, while the maximum number of steps were increased from 1000 to the maximum of 9,999,9999. This was done to ensure the lowest number of repeating conformers, or duplicates, while also having an accurate and consistently high output of conformers.

These minimizations were carried out until the number of conformers outputted were stabilized. The rotational bonds are set on the dippe ligand backbone and P—C bonds as shown in red in **Figure 14**. The conformers will be rotating around the P(2)-Ni1)-P(3) bond, the dihedral angles are identified as Ni(1)-P(2)-C(8)-H(9), Ni(1)-P(3)-C(44)-H(45), P(2)-C(24)-C(27)-P(3), Ni(1)-P(2)-C(18)-H(19), Ni(1)-P(3)-C(34)-H(35), shown in **Figure 15**. Around 244 structures were calculated using MM calculations, these structures are overlaid, as shown in **Figure 16**.

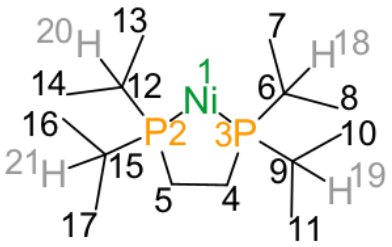

Figure 14: The [Ni(dippe)] Fragment structure with a focus on the square planar formation of Ni(1)-P(2)-P(3)-C(4)-C(5), the 7 rotatable bonds shown in Red, the Nickel is shown in green, the Phosphorous are shown in tangerine, the important Hydrogens are shown in gray, and the carbons are left as black.

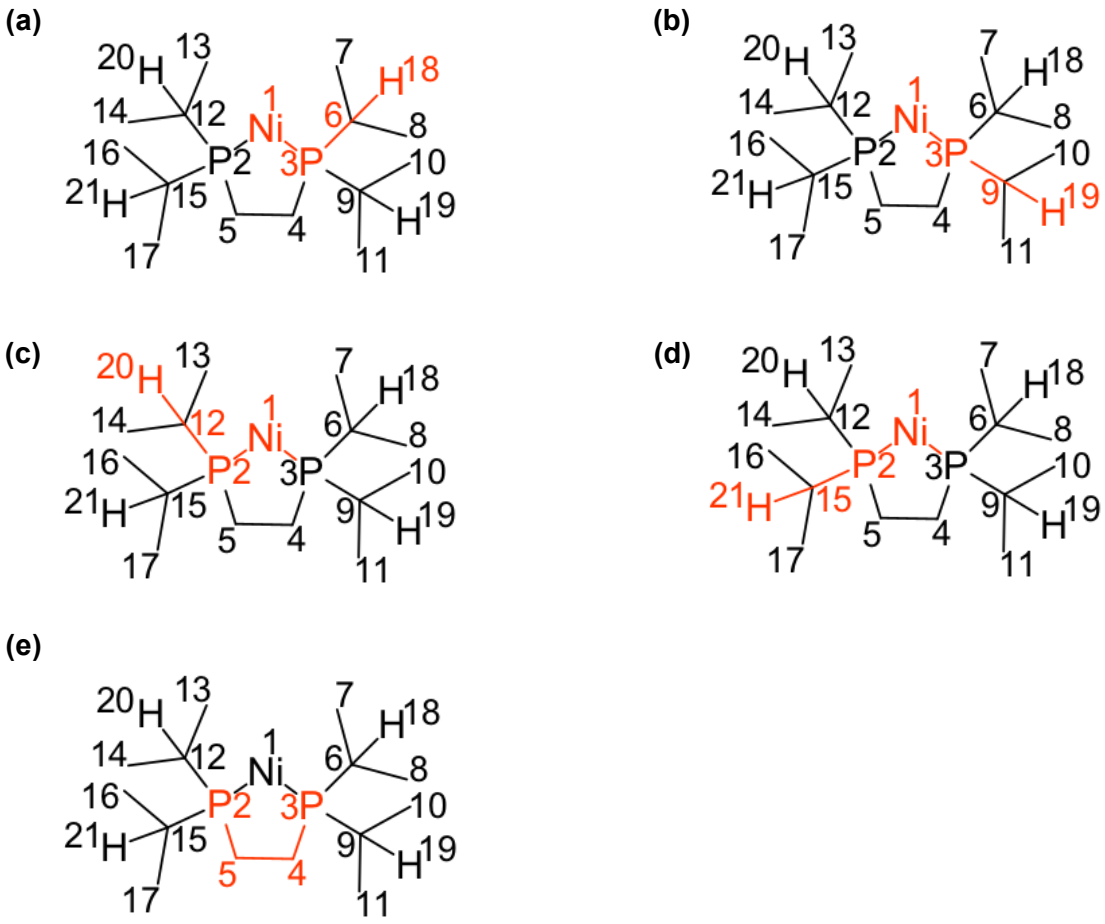

Figure 15: The Fives different dihedral angles of [Ni(dippe)]_1, Ni(1)-P(3)-C(6)-H(18), Ni(1)-P(3)-C(9)-H(19), Ni(1)-P(2)-C(12)-H(20), Ni(1)-P(2)-C(15)-H(21) , P(2)-C(5)-C(4)-P(3).

(a)

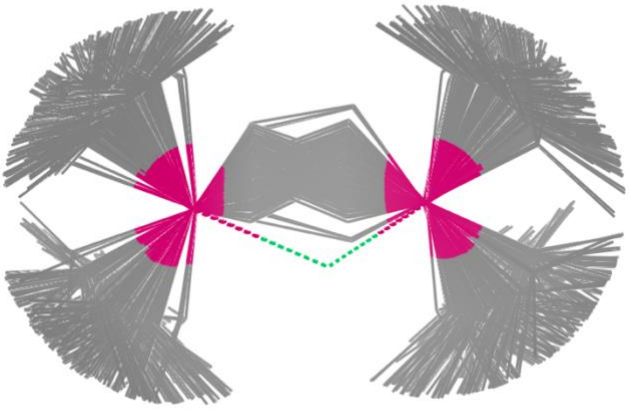

(b)

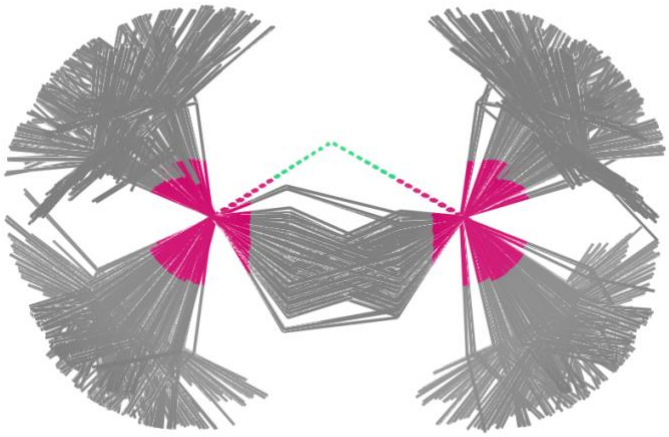

Figure 16: 244 conformers of the [Ni(dippe)] Fragment overlaid in Schrodinger Macromodel. This is prior to optimization and further removal of duplicates.

Optimization performed using QM Methods with DFT calculations

The DFT calculations were benchmarked to determine the best parameters and constraints. The benchmark covered various parameters and concluded that the function B3LYP performed the best for [Ni(dippe)] fragment calculations, as shown in **Table 1**.[46]

Table 1: Reported energies for H_2 of the best performing parameters for [Ni(dippe)] Fragment. ΔG is reported in kcal/mol calculated by Gaussian16, C, H (6-31G**); Ni, P (SDDALL), α(Ni)= 3.130, α(P) = 0.387.[45]

	DG (thf)	DG (tol)	DG(thf)/DG(tol)
Expt	-1.16	-0.51	2.3
B3LYP-GDBJ3	-8.26	-3.61	2.3
B3LYP-GD3 (qh)	-7.72	-3.20	2.4
CAM-B3LYP GD3 (qh)	-7.89	-3.20	2.5
B3LYP	-1.00	2.90	-0.3
M06	-2.22	1.63	-1.4
M06-GD3 (qh)	-4.32	-0.11	37.8

Gaussian 16 suite of program was used to perform all of the quantum mechanical calculations.[47] The starting geometry of [Ni(dippe)] fragment and the lowest energy conformers found by MM method were fully optimized in redundant internal coordinates without any symmetry constraints with Density Functional Theory (DFT) and a wave function incorporating the hybrid function of Becke's three-parameter (B3), along with Lee-Yang-Parr correlation functional (LYP) with Grimme's GD3 dispersion corrections.[48,49] Corrected energies and dihedral angles were calculated using the polarization function 6-31G** for C and H and SDDALL basis sets with the effective core pseudopotentials improved with a set of f-polarization functions for Ni (α = 1.472)[50] and a set of d-polarization functions for P (α = 0.387)[51]. The geometries were fully optimized with ultrafine integration grid sizes and tight convergence criteria. The Solvent Model Density (SMD) calculations were done with toluene as a model for the solvent effects on the geometries and the relative stabilities of the conformers. Single-point energy calculations on the

optimized geometries were performed using the DFT hybrid function (with GD3 dispersion correct) with the same basis set as detailed above for Ni and P, and the polarized and diffused 6-311++ basis set for all of the other atoms.[49,50]

Even after optimization, the possibility of duplicates persisting is imminent. Therefore, duplicates must be removed to ensure accurate data. This process is demonstrated in the graphic shown below in **Figure 17**. The conformers are separated according to three different regions based off of their dihedral angles, these regions are the angles: Region A being -180˚ to -120˚and 120˚ to 180˚, Region B being -120˚ to 0˚, and Region C being 0˚ to 120˚. Once the conformers are correctly identified and separated they are then labelled according to their backbone, δ or λ, orientation and five different dihedral angles, this labelling is based off on John Gladysz's paper octahedral Werner complexes.[52] Finally, any conformers that had a matching identity and energy to an already existing conformer will be eliminated.

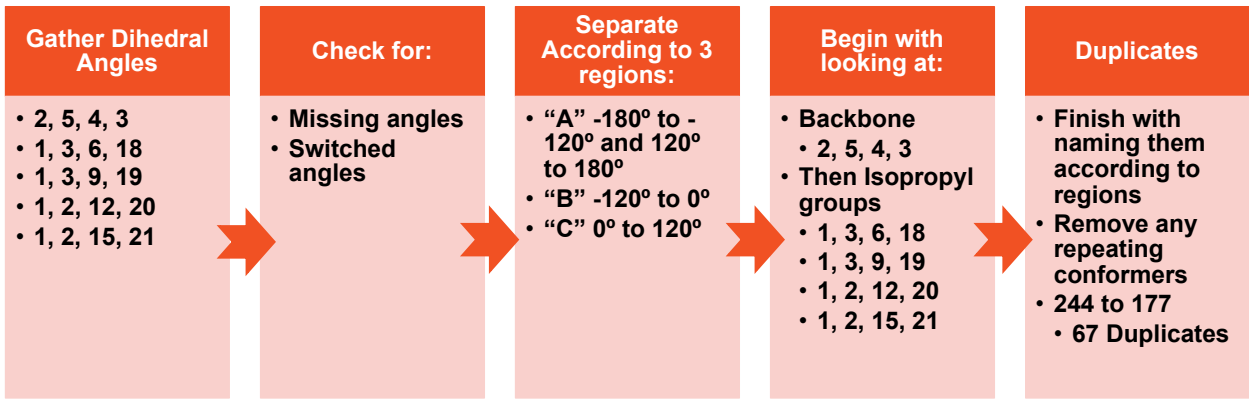

Figure 17: The process of removing duplicating conformers that remained after optimization.

CHAPTER IV

RESULTS AND DISCUSSION

The conformational search of [Ni(dippe)] fragment generated 244 conformers. The conformers were calculated through the use of MM calculations, where it was then overlaid using Schrodinger Macromodel prior to removing duplicates. The (a) front view and (b) back view can be seen in **Figure 16**, where the Nickel is shown in green, the phosphor in pink, the carbons in gray, and the hydrogens omitted for clarity. The overlay outlines the isopropyl groups rotation, as well as the P-C-C-P backbone dihedral angle change. After removing the duplicates, the number of conformers decreased to 177.

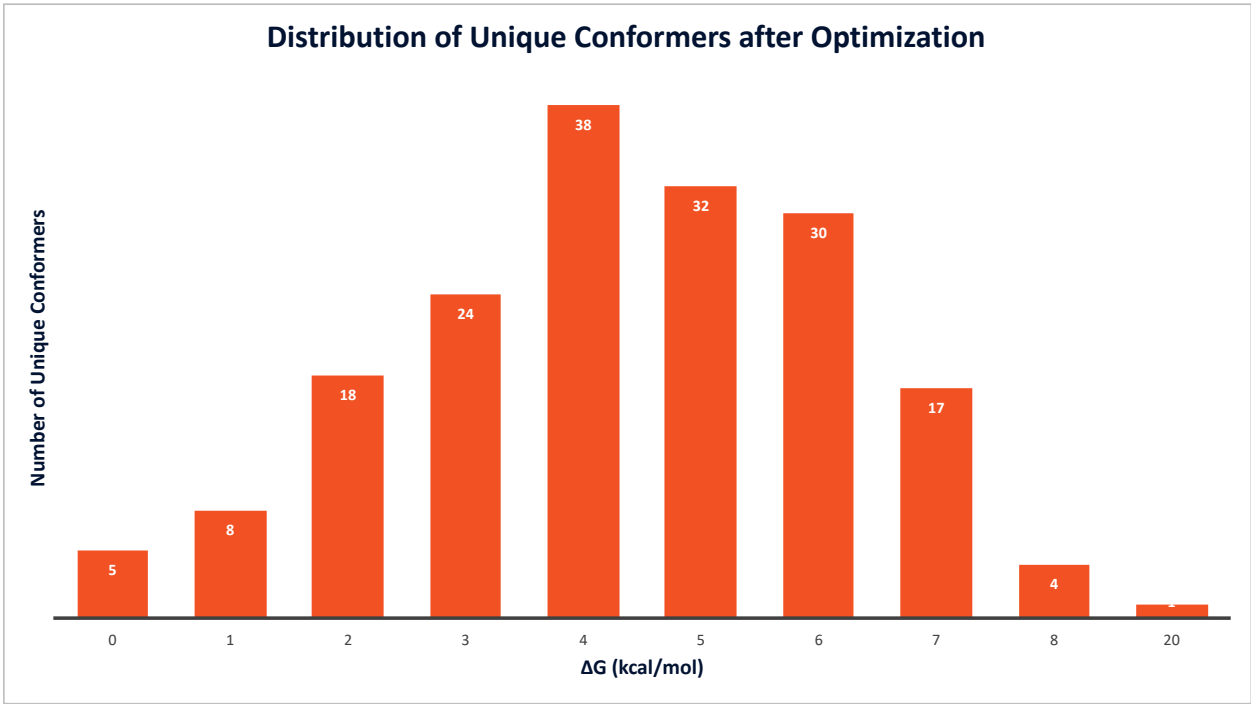

Figure 18: Energy distribution of [Ni(dippe)] conformers. ΔG is in kcal/mol.

A percent population was taken to determine which percent of conformers should be studied heavily. It was found that the five lowest energy conformers from 0.0 kcal/mol to 1.0 kcal/mol made up around 72.0% of the conformers. **Table 2** shows a more detailed breakdown of the percent population for the five lowest energy conformers, where the lowest energy conformer at 0.0 kcal/mol made up 29.2% of the conformer population, and as the energy increased the percent population of that conformer decreased.

Table 2: The relative energies and the percent population of 5 lowest energy conformers.

ΔG (kcal)	%
0.0	15.5
0.1	13.1
0.2	11.1
0.3	9.4
0.4	7.9
0.5	6.7
0.6	5.6
0.7	4.8
0.8	4.0
0.9	3.4
1.0	2.9

The Calculation that was done to find the percent population is as followed:

Calculation for Percent Population of 5 lowest energy conformers:

Using the equation:

$$\frac{N_i}{N} = \frac{g_i e^{-\beta \Delta G_i}}{\sum g e^{-\beta \Delta G}} \qquad \textbf{(Equation 1)}$$

Where *i* represents the initial conformer that is being observed, *g* is the degeneracy, k_B is the Boltzmann constant in kcal/mol, ΔG is the energy of the conformer in kcal/mol, and β can be represented as, where T is in Kelvins:

$$\beta = \frac{1}{k_B T} \qquad \textbf{(Equation 2)}$$

Using **Equation 1**, the percent was calculated and is shown in **Table 2**.

All 177 conformers were then organized by their isopropyl group configuration, backbone, and number of conformers, as seen in **Table 3**. The conformers themselves are

grouped according to their mirror or pseudo-mirror conformers, for example δaaaa is the pseudo-mirror isomer of λaaaa.

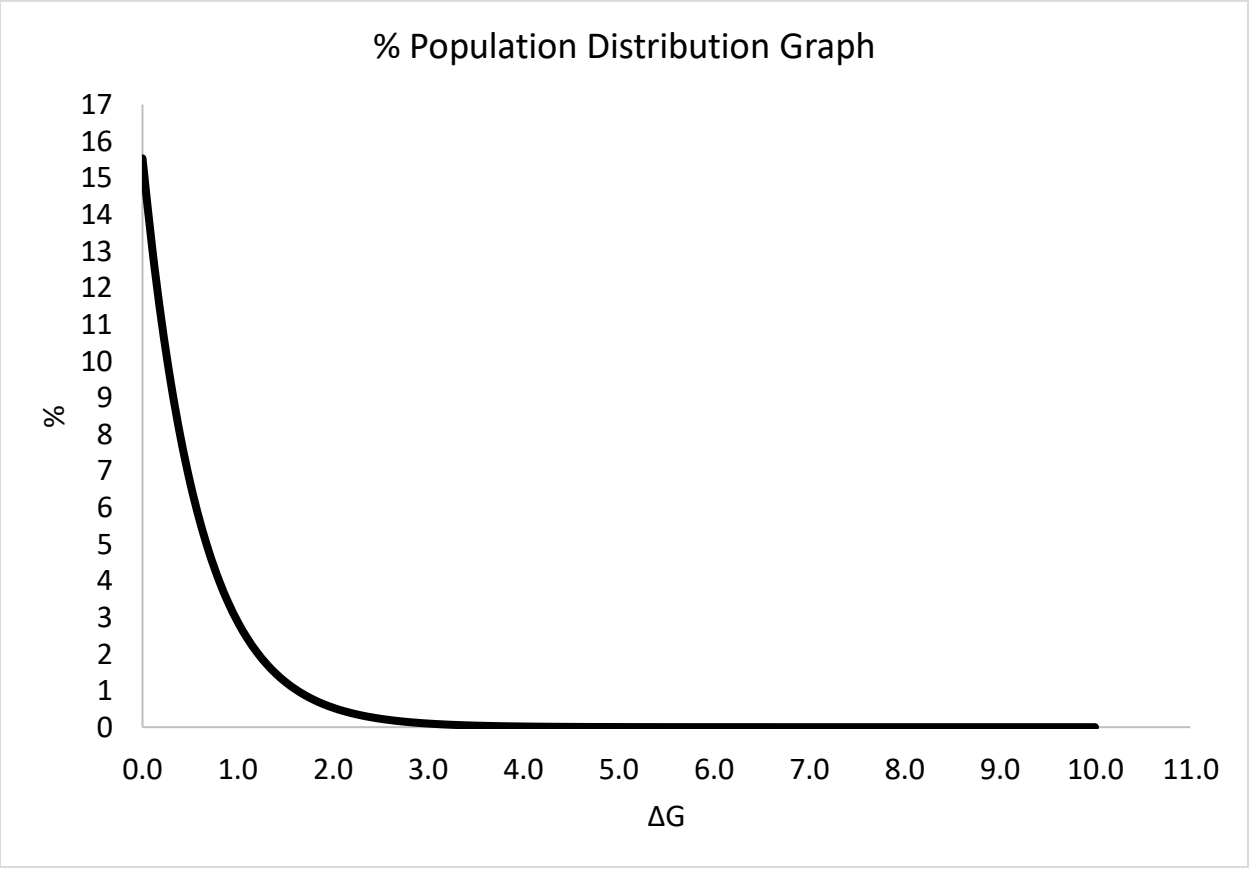

Figure 19: Percent population distribution graph showing the most occupied population is located between 0.0 to 1.0 kcal/mol.

The percent population distribution of the unique conformers is represented in **Figure 19**, where the bulk of the conformers are located between 0.0kcal/mol to 1.0kcal/mol. Therefore, we can disregard any conformers with an energy greater than 1.0kcal/mol because it is unrepresentative of the population.

Table 3: Conformation angles classifications for the isopropyl dihedral angles Ni-P-C-H.

***i*-Pr Dihedral Angle Classification *i*-Pr Dihedral Angle Classification**		
Ni-P-C-H	**Angle**	**Abbreviations**
-180° to -130° from 130° to 180°	Anti-periplanar	a
-110° to 10°	Gauche (-)	g^-
10° to 110°	Gauche (+)	g^+

Table 4: Isopropyl groups and dihedral angle configuration for the [Ni(dippe)] fragment conformers.

***i* – Pr Group Configuration**	**Back bone**	**Number of Conf.**	**ΔG Range**
aaaa aaaa	δ λ	4	4.0 – 4.8
$aaag^-$ g^-aaa g^+aaa ag^-aa g^+aaa ag^+aa ag^-aa aag^+a	δ λ	12	2.1 – 4.4
g^-ag^-a g^-ag^+a g^-aag^- g^-g^-aa g^-g^+aa g^-aag^+ g^-g^+aa g^+ag^-a g^+ag^+a ag^+ag^+ ag^-ag^+ ag^+g^+a g^-g^+aa g^-g^+aa ag^+g^-a g^-g^+aa ag^+ag^- ag^-ag^-	δ λ	40	0.0 – 6.9
g^+aag^- g^+g^-aa g^+g^+aa ag^+g^-a ag^+g^+a ag^+ag^- ag^+ag^+ aag^+g^- ag^-g^+a g^+g^-aa g^-g^-aa ag^+g^-a g^+aag^+ g^-ag^+a g^-ag^-a aag^+g^-	δ λ		
$g^-ag^-g^-$ $g^-ag^-g^-$ $g^-g^-g^+a$ $g^-g^-ag^+$ $g^-g^-ag^-$ $g^-g^+g^+a$ $g^-g^+g^-a$ $g^+g^+ag^+$ $ag^+g^+g^+$ $g^+g^+ag^-$ $g^+g^+g^-a$ $g^+g^+g^+a$ $g^-g^+ag^-$ $g^-g^+ag^+$	δ λ	56	2.3 – 6.1
$g^+g^+g^-a$ $g^+g^+g^+a$ $g^+g^+ag^-$ $g^+g^+ag^+$ $ag^-g^-g^-$ $ag^-g^+g^-$ $ag^-g^+g^+$ $g^-g^-ag^+$ $g^-g^-ag^-$ $g^-g^-g^+a$ $g^-g^-g^-a$ $g^+ag^+g^+$ $g^+ag^+g^-$ $g^+ag^-g^-$	δ λ		
$g^-g^+ag^-$ $g^+g^-g^+a$ $g^+g^-ag^-$ $g^+g^-ag^+$ ag^-ag^- $ag^+g^-g^-$ $ag^+g^+g^-$ $g^-g^+g^+a$ $g^+g^-ag^-$ $g^+g^-g^+a$ $g^+g^-g^-a$ g^+ag^+a $g^-ag^+g^+$ $g^-ag^+g^-$	δ λ		
$g^-g^-g^+g^-$ $g^-g^-g^+g^+$ $g^-g^+g^-g^-$ $g^-g^+g^+g^-$ $g^-g^+g^-g^+$ $g^-g^+g^+g^+$ $g^+g^+g^+g^-$ $g^-g^-g^+g^+$ $g^-g^+g^+g^+$ $g^-g^+g^+g^-$ $g^-g^+g^-g^+$ $g^-g^+g^-g^-$	δ λ	44	4.5 – 8.6
$g^+g^-g^-g^+$ $g^+g^-g^+g^-$ $g^+g^-g^+g^+$ $g^+g^+g^-g^-$ $g^+g^+g^-g^-$ $g^+g^+g^-g^+$ $g^+g^+g^+g^-$ $g^+g^-g^-g^+$ $g^+g^-g^+g^-$ $g^+g^-g^-g^-$ $g^+g^+g^-g^-$ $g^-g^-g^+g^+$ $g^-g^-g^-g^+$ $g^-g^-g^+g^-$	δ λ		
$g^-g^-g^-g^-$ $g^+g^+g^+g^+$ $g^+g^+g^+g^+$ $g^-g^-g^-g^-$	δ λ	8	5.0 – 6.9

The percent population distribution of the unique conformers is represented in **Figure 19**, where the bulk of the conformers are located between 0.0 kcal/mol to 1.0 kcal/mol. Therefore, we can disregard any conformers with an energy greater than 1.0 kcal/mol because it is unrepresentative of the population.

The isopropyl groups for the dihedral angles were then classified and separated according to **Table 3**. For our system, the lowest energy conformer is represented as gauche (+), g^+, and gauche (-), g^-, due to the hydrogen being in closer proximity to the nickel metal center. While the anti-periplanar angle exhibits higher energy because the methyl groups are sterically crowded around the nickel metal center. The conformers are then separated according to how many gauche angles they have, which is represented in **Table 4**. The *i*-Pr group configuration are grouped according to pseudo-mirror images, where the δ backbone is on top of the paired λ backbone. These mirror images do not have the same energies, due to possible error within the basis sets, but can still be considered mirror images due to *i*-Pr configurations. The largest group were the conformers that contained three gauche angles, while the lowest energy conformers can be found with group that contained only two gauche angles. Currently, there is no correlation between the energy range exhibited by the grouped conformers. This is because the ΔG range is too wide for each group and they also overlap, for example, the group with three gauche angles have a range between 2.3 – 6.1 kcal/mol, which overlaps with the group of conformers that have an energy range of 0.0 – 6.9 kcal/mol.

Table 5: Dihedral angles of the isopropyl groups and backbone for the five lowest energy conformers.

File Name	ΔG(kcal/mol)	1,2,12,20	1,2,15,21	1,3,9,19	1,3,6,18	2,5,4,3	Config.
Nidippe1	0.00	-82.99	-158.07	-82.78	-157.12	-39.84	$g^{-}ag^{-}a$ δ
Nidippe2	0.16	157.80	82.72	157.84	82.67	39.51	$ag^{+}ag^{+}$ λ
Nidippe4	0.80	150.30	77.41	-82.53	-157.15	-40.54	$ag^{+}g^{-}a$ δ
Nidippe29	0.80	158.26	82.72	-77.61	-150.41	40.51	$ag^{+}g^{-}a$ λ
Nidippe15	0.99	-150.56	-77.02	157.68	82.63	40.61	$g^{+}aag^{-}$ λ

The five lowest energy conformers, along with their energy, dihedral angles, and *i*-Pr configuration can be seen in **Table 5**. In the lowest two energy conformers, Nidippe1 and Nidippe2, the backbones mirror each other, where Nidippe1 exhibits a δ backbone configuration. The lowest energy conformer is shown in **Figure 20**, where the square planar structure remained constrained, the gauche and antiperiplanar configuration correspond with **Table 5.** The lowest energy conformer adhered to a C_2 point group, which can be seen in **Figure 21**.

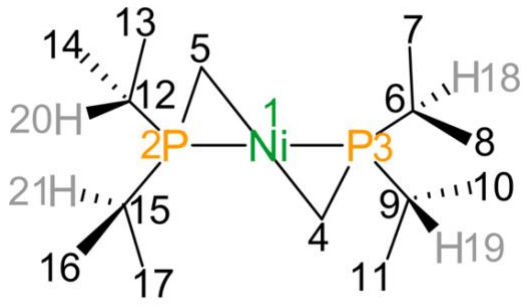

Figure 20: The Lowest Energy Conformer, with a Configuration of $g^{-}ag^{-}a$ δ and energy of ΔG = 0.0 kcal/mol.

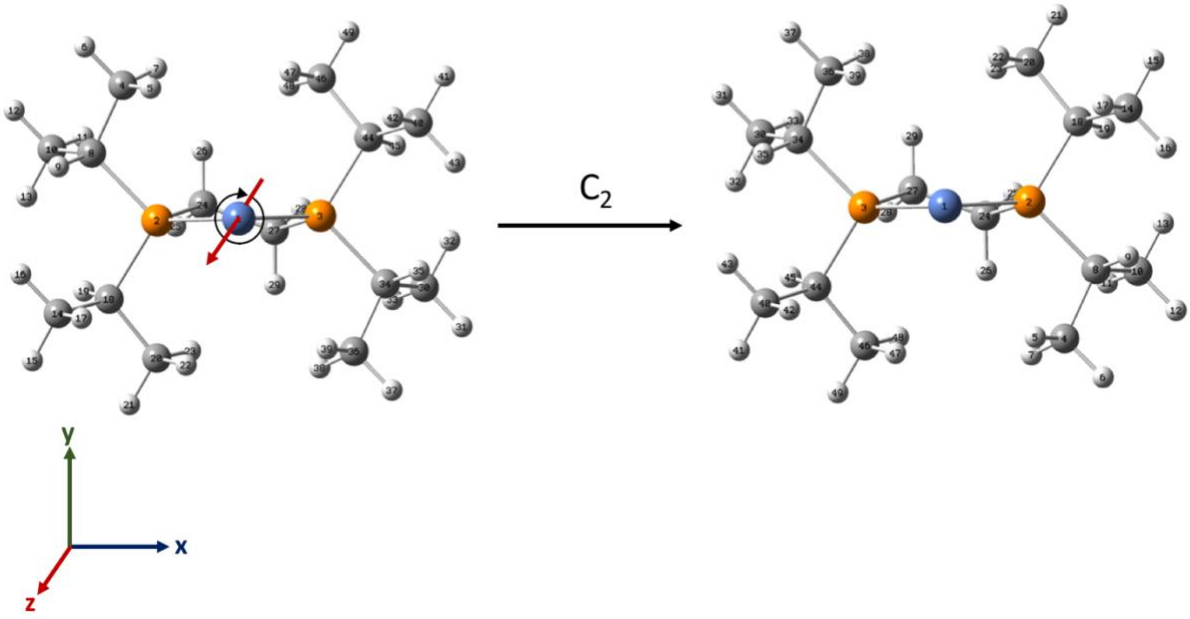

Figure 21: The lowest energy conformer displays C_2 symmetry, the nickel atom is shown in blue, the phosphor atoms are shown in orange, the carbon atoms are shown in grey and the hydrogens are shown in white.

The second lowest energy conformer, 0.2 kcal/mol and exhibits C_2 symmetry as well, mirrors the lowest energy conformer. The first lowest energy conformer takes the configuration of $g^{-}ag^{-}a\ \delta$, the second lowest energy conformer takes the configuration of $ag^{+}ag^{+}\ \lambda$ which is visually confirmed in **Figure 22**. Where the isopropyl groups and backbone reflects the same atom, but the carbons are numerically labelled differently. This could be because they rotated during the optimization calculations, therefore this will need to be further studied and reoptimized to ensure these carbons are rotating within the isopropyl groups. The geometry in these two conformers were also observed in the crystal structures from Jones group.[14]

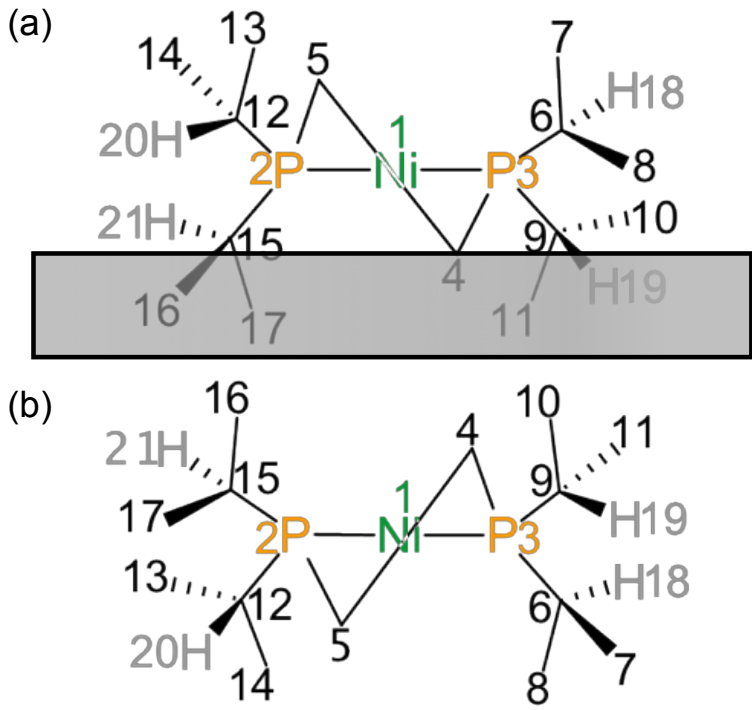

Figure 22: The comparison of two lowest energy conformers of [Ni(dippe)] fragment. (a) front view of lowest conformer generated with a ΔG=0.0 kcal/mol and (b) second lowest conformer with a ΔG=0.2 kcal/mol both exhibit C_2 symmetry.

A comparison of the lowest energy conformer with the third lowest energy conformer is shown in **Figure 23**. The left side of both molecules are different from each other, but the backbone and right side of the molecules are identical. The hydrogens stereochemistry switches, where H(20) goes from in-plane for the lowest energy conformer to out-of-plane for the third lowest energy conformer, the energy difference is 0.8 kcal/mol which can be accounted for in the left side of the molecules.

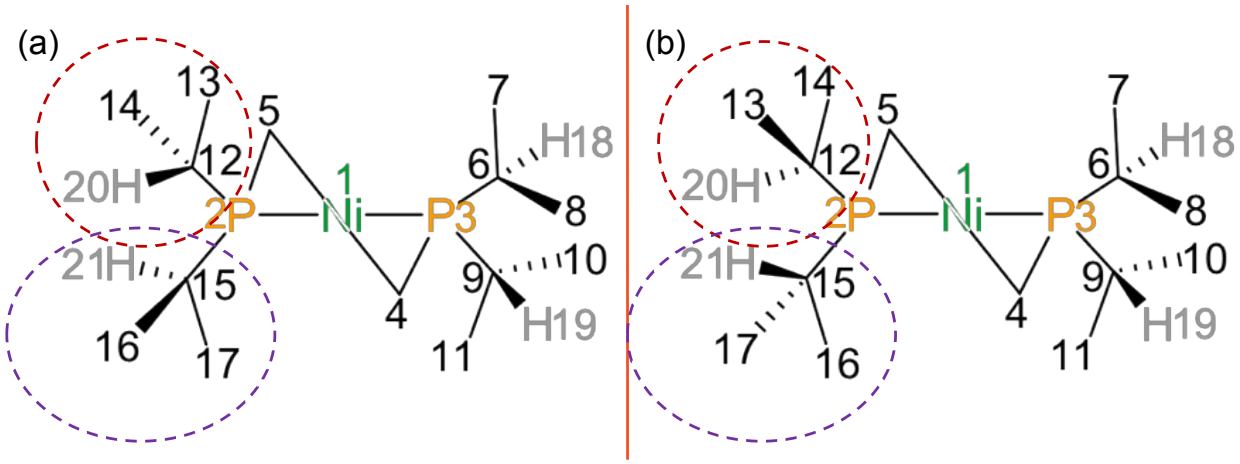

Figure 23: The comparison of the lowest energy conformer of [Ni(dippe)] fragment with the third lowest energy conformer. (a) front view of lowest conformer generated, Nidippe1, with a ΔG=0.0 kcal/mol and (b) third lowest conformer, Nidippe4, with a ΔG=0.8 kcal/mol. (A pseudo-mirror image).

A comparison of the fourth and the third lowest energy conformers are shown in **Figure 24.** Like the first two lowest energy conformers they are also mirror image of one another, except for the backbone, with an energy difference of 0.2 kcal/mol. The fourth lowest energy conformer takes a configuration of ag^+g^-a λ and the third lowest energy conformer takes the configuration of ag^+g^-a δ which can be seen visually in **Figure 24**. Where the backbones mirror each other, similar to the first and second lowest energy conformer. While the isopropyl groups do not mirror each other but remain unchanged which can account for the minimal energy difference.

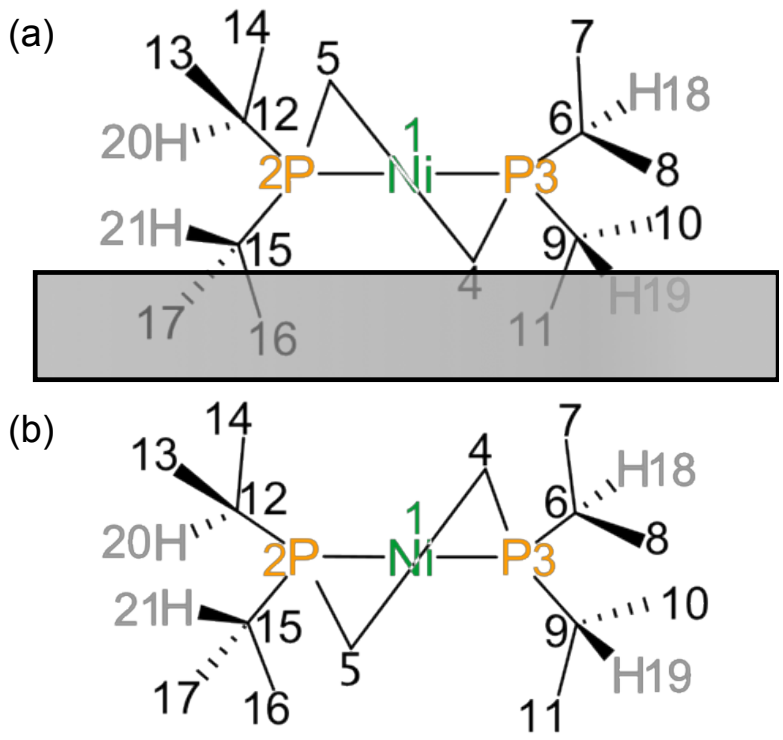

Figure 24: The comparison of the fourth and the third lowest energy conformers of [Ni(dippe)] fragment, respectively. (a) A front view of fourth lowest energy conformer generated with a ΔG=0.8 kcal/mol and (b) a fifth lowest energy conformer with a ΔG=1.0 kcal/mol.

The third lowest energy conformer left side of the molecule and backbone mirror each other while the right side is completely different, shown in **Figure 25.** Like the other mirror images, these molecules are not true isomers or mirror images of one another due to the difference in energy. This may have risen from the optimization portion of the calculations, where there the need for more constraints might be necessary to achieve accurate energy data while still being computationally efficient.

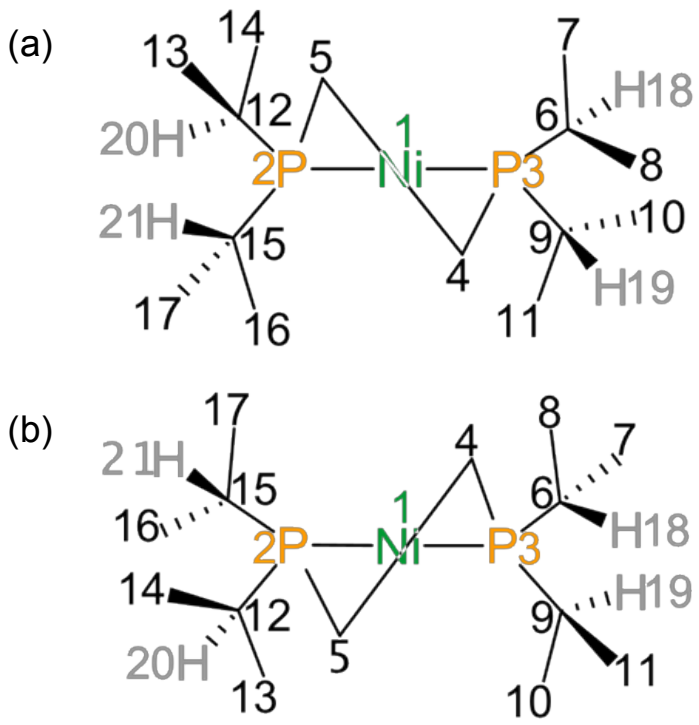

Figure 25: A comparison of (a) the third lowest energy conformer, Nidippe4, with an energy of ΔG= 0.8 kcal/mol (b) and the fifth lowest energy conformer, Nidippe15, with an energy of ΔG= 1.0 kcal/mol.

CHAPTER V

CONCLUSION

The conformational search of the [Ni(dippe)] fragment was thorough, but a stricter optimization may need to be performed to achieve better energy results. While the energy may be slightly different for the pseudo-mirror images, it was noted in Jensen's "Introduction to Computational Chemistry," that the error for energies can typically margin around 4 kcal/mol to 1 kcal/mol depending on how "balanced" the basis set is. Therefore, if the error is as constant as possible then it may be negated. While this error is present, the lowest energy conformer still exhibited a C_2 symmetry which was mirrored by the second lowest energy conformer. This also matched with the crystal structures in Jones paper. It was also found that the group of conformers that contained two gauche angles contained the five lowest energy conformers. The five lowest energy conformers also made up more than 80% of the population. This work will be used in the future for a study between [Ni(dippe)], [Pt(dippe)], and [Pd(dippe)] for reactions regarding C–CN bond activation with and without Lewis-acid.

CHAPTER VI

FUTURE WORK

A future study will be done where the conformers will be re-optimized, including single point energy (SPE) calculations, and focusing on less than 100 frequencies. Other optimization functions that will be regarded include the tight optimization, ultrafine grid, solvation, empirical dispersion, and Quasi harmonic approximation. This will be done to minimize error as much as possible and to allow the conformer to be true mirror images instead of pseudo-mirror images. A DFT analysis where Lewis-acid assisted C–CN bond activation using [M(dippe)], where M= Ni, Pd, Pt, in benzonitrile and acetonitrile is underway. Where Natural bond order (NBO) and Atom-in-Molecules (AIM) calculations are also being performed.

REFERENCES

1. Clevenger, A. L., Stolley, R. M., Aderibigbe, J., & Louie, J. (2020). Trends in the Usage of Bidentate Phosphines as Ligands in Nickel Catalysis. *Chemical Reviews*, *120*(13), 6124 – 6196. DOI: https://dx.doi.org/10.1021/acs.chemrev.9b00682.

2. McRae, M., 2022, Nickel Statistics and Information – by National Minerals Information Center: *U.S. Geological Survey*, Accessed April 3, 2022, at https://www.usgs.gov/centers/national-minerals-information-center/nickel-statistics-and-information

3. Ananikov, V. P. (2015). Nickel: The "Spirited Horse" of Transition Metal Catalysis. *ACS Catalysis*, *5*(3),1964 – 1971. DOI: https://doi.org/10.1021/acscatal.5b00072.

4. Zhang, Y. (1982). Electronegativities of Elements in Valence States and Their Applications. 1. Electronegativities of Elements in Valence States. *Inorganic Chemistry*, *21*(11), 3886 – 3889. DOI: https://doi.org/10.1021/ic00141a005.

5. Keyan, L., & Xue, D. (2006). Estimation of Electronegativity Values of Elements in Different Valence States. *The Journal of Physical Chemistry A*, *110*(39), 11332 – 11337. DOI: https://doi.org/10.1021/jp062886k.

6. Irving, H., Williams, R. J. P. (1953). The Stability of Transition-Metal Complexes. *Journal of Chemical Society*, 3192 – 3210. DOI: https://doi.org/10.1039/JR9530003192.

7. Tasker, S. Z., Standley, E. A., Jamison, T. F. (2014). Recent Advances in Homogeneous Nickel Catalysis, *Nature*, *509*, 299 – 309. DOI: https://doi.org/10.1038/nature13274.

8. Martin, R., Buchwald, S. L. (2008). Palladium-Catalyzed Suzuki−Miyaura Cross-Coupling Reactions Employing Dialkylbiaryl Phosphine Ligands, *Acc. Chem. Res., 41*(11), 1461 – 1473. DOI: https://doi.org/10.1021/ar800036s.

9. **Tolman References: (a)** Tolman, C. A. (1970). Electron donor-acceptor properties of phosphorus ligands. Substituent additivity. *J. Am. Chem. Soc., 92*, 2953 – 2956. DOI: https://doi.org/10.1021/ja00713a006. **(b)** Tolman, C.A. (1977). Steric effects of phosphorus ligands in organometallic chemistry and homogeneous catalysis. *Chem. Rev., 77*, 313 – 348. DOI: https://doi.org/10.1021/cr60307a002.

10. Sajith, P. K., Suresh, C. H. (2011). Mechanism of Reductive Eliminations in Square Planar Pd(II) Complexes: Nature of Eliminated Bonds and Role of *Trans* influence, *Inorg. Chem.*, *50*(17), 8085 – 8093. DOI: https://doi.org/10.1021/ic2004563.

11. Kranenburg, M., Kamer, P. C. J., van Leeuwen, P. W. N. M., Vogt, D., Keim, W. (1995). Effect of the bite angle of diphosphine ligands on activity and selectivity in the nickel-catalyzed hydrocyanation of styrene, *J. Chem. Soc., Chem. Commun*., 2177 − 2178. DOI: https://doi.org/10.1039/C39950002177.

12. Goertz, W., Kamer, P. C. J., Van Leeuwen, P. W. N. M., Vogt, D. (1997). Application of chelating diphosphine ligands in the nickel-catalyzed hydrocyanation of alk-l-enes and ω-unsaturated fatty acid esters, *Chem. Commun.*, 1521 − 1522. DOI: https://doi.org/10.1039/A702811C.

13. Zuidema, E., van Leeuwen, P. W. N. M., Bo, C. (2005). Reductive Elimination of Organic Molecules from Palladium-Diphosphine Complexes, *Organometallics*, *24*(15), 3703 – 3710. DOI: https://doi.org/10.1021/om050113x.

14. X-ray crystal structures: (a) Swartz, B. D., Brennessel, W. W., Jones, W. D. (2018). Lewis Acid Assisted C–CN Cleavage of Benzonitrile Using [(dippe)NiH]$_2$, *Synlett*, *29*, 747 – 753. DOI: https://doi.org/10.1055/s-0036-1590801. (b) Ting, L., Garcia, J. J., Brennessel W. W., Jones, W. D. (2010). C–CN Bond Activation of Aromatic Nitriles and Fluxionality of the η^2-Arene Intermediates: Experimental and Theoretical Investigations, *Organometallic*, *29*, 2430 – 2445. DOI: https://doi.org/10.1021/om100001m.

15. Huang, J., Haar, C. M., Nolan, S. P., Marcone, J. E., Moloy, K. G. (1999). Lewis Acids Accelerate Reductive Elimination of RCN from P_2Pd(R) (CN), *Organometallics*, *18*(3), 297 – 299. DOI: https://doi.org/10.1021/om980897x.

16. Wolters, L. P., Koekkoek, R., Bickelhaupt, F. M. (2015). Role of Steric Attraction and Bite-Angle Flexibility in Metal-Mediated C–H Bond Activation, *ACS Catal., 5*(10), 5766 – 5775. DOI: https://doi.org/10.1021/acscatal.5b01354.

17. Thorn, D. L., Hoffmann, R. (1978). The Olefin insertion reaction. *J. Am. Chem. Soc.*, *100*(7), 2079 – 2090. DOI: https://doi.org/10.1021/ja00475a018.

18. Ge, S., Green, R. A., Hartwig, J. F. (2014). Controlling First-Row Catalysts: Amination of Aryl and Heteroaryl Chlorides and Bromides with Primary Aliphatic Amines Catalyzed by a BINAP-Ligated Single- Component Ni(0) Complex, *J. Am. Chem. Soc.*, *136*(4), 1617 − 1627. DOI: https://doi.org/10.1021/ja411911s.

19. Murakami, M., Itahashi, T., Ito, Y. (2022). Catalyzed Intramolecular Olefin Insertion into a Carbon−Carbon Single Bond, *J. Am. Chem. Soc.*, *124*(47), 13976 – 13977. DOI: https://doi.org/10.1021/ja021062n.

20. **For further reading on dippe ligand in the Jones group: (a)** Garcia, J. J., Brunkan, N. M., Jones, W. D. (2022). Cleavage of Carbon−Carbon Bonds in Aromatic Nitriles Using Nickel(0), *J. Am. Chem. Soc.*, *124*(32), 9547 – 9555. DOI: https://doi.org/10.1021/ja0204933. **(b)** Kundu S., Snyder B. E. R., Walsh A. P., Brennessel W. W., Jones W.D. (2013). C–S bond activation of thioethers using (dippe)Pt(NBE)$_2$, *Polyhedron*, *58*, 99 – 105. DOI: https://doi.org/10.1016/j.poly.2012.07.071. **(c)** Ateşin T. A., Li T., Lachaize S., García J. J., Jones W. D. (2008). Experimental and theoretical examination of C-CN bond activation of benzonitrile using zerovalent nickel, *Organometallics*, *27*(15), 3811-3817. DOI: https://doi.org/10.1021/om800424s. **(d)** Ateşin T. A., Li T., Lachaize S., Brennessel W. W., García J. J., Jones W. D. (2007). Experimental and theoretical examination of C–CN and C–H bond activations of acetonitrile using zerovalent nickel, *J. Am. Chem. Soc*., *129*(24), 7562 – 7569. DOI: https://doi.org/10.1021/ja0707153.

21. **For further reading on dmpe ligand: (a)** Hsu G. C., Kosar W. P., Jones W. D. (1994). Functionalization of benzylic carbon-hydrogen bonds. Mechanism and scope of the catalytic synthesis of indoles with [Ru(dmpe)$_2$], *Organometallics*, *13*(1), 385 – 396. DOI: https://doi.org/10.1021/om00013a056. **(b)** Hall C., Jones W. D., Mawby R. J., Osman R., Perutz R. N., Whittlesey M. K. (1992). Matrix isolation and transient photochemistry of ruthenium complex Ru(dmpe)$_2$H$_2$: characterization and reactivity of Ru(dmpe)$_2$ (dmpe = Me$_2$PCH$_2$CH$_2$PMe$_2$), *J. Am. Chem. Soc.*, *114*(19), 7425 – 7435. DOI: https://doi.org/10.1021/ja00045a014.

22. **Garcia et. al. use of [Ni(dippe)]: (a)** Garcia-Ventura I., Flores-Alamo M., Garcia J. J. (2016). Carbon–carbon vs. carbon–oxygen bond activation in 2- and 3-furonitriles with nickel, *RSC Adv., 6*(103), 101259 – 101266. DOI: https://doi.org/10.1039/C6RA20244F. **(b)** Gutierrez-Ordaz, R., Garcia, J. J. (2018). Desulfurization of dibenzothiophene and dibenzothiophene sulfone via Suzuki–Miyaura type reaction: Direct access to o-terphenyls and polyphenyl derivatives, *Polyhedron*, *154*, 373 – 381. DOI: https://doi.org/10.1016/j.poly.2018.08.008. Reprinted from Polyhedron, 154, Gutiérrez-Ordaz, R. and García J. J., Desulfurization of dibenzothiophene and dibenzothiophene sulfone via Suzuki–Miyaura type reaction: Direct access to *o*-terphenyls and polyphenyl derivatives, 378 –381, Copyright (2018), with permission from Elsevier. **(c)** Castellanos-Blanco, N., Flores-Alamo, M., Garcia, J. J. (2015). Tandem hydrogenation and condensation of fluorinated α,β-unsaturated ketones with primary amines, catalyzed by nickel, *Dalton Transaction*, *44*(35), 15653 – 15663. DOI: https://doi.org/10.1039/C5DT02366A.

23. Crabtree, Robert H. *The Organometallic Chemistry of the Transition Metals*. J. Wiley, 2014.

24. Ang, M. L., Oemar, U., Saw, E. T., Mo, L., Kathiraser, Y., Chia, B. H., Kawi, S. (2014). Highly Active Ni/xNa/CeO2 Catalyst for the Water–Gas Shift Reaction: Effect of Sodium on Methane Suppression, *ACS Catal.*, *4*(9), 3237 – 3248. DOI: https://doi.org/10.1021/cs500915p.

25. Jover, J., Miloserdov, F. M., Benet-Buchholz, J., Grushin, V. V., Maseras, F. (2014). On the feasibility of nickel-catalyzed trifluoromethylation of aryl halides, *Organometallic*, *33*(22), 6531 – 6543. DOI: https://doi.org/10.1021/om5008743.

26. Muetterties, E. L., Gerlach, D. H., Kane, A. R., Parshall, G. W., Jesson J. P. (1971). Reactivity of trialkylphosphine complexes of platinum(O), *J. Am. Chem. Soc.*, *93*(14), 3543 – 3544. DOI: https://doi.org/10.1021/ja00743a050.

27. Halpern, J. (1982). Determination and significance of transition metal-alkyl bond dissociation energies, *Acc. Chem. Res.*, *15*(8), 238 – 244. DOI: https://doi.org/10.1021/ar00080a002.

28. Souillart, L.; Cramer, N. (2015). Catalytic C–C Bond Activations via Oxidative Addition to Transition Metals, *Chem. Rev.*, *115*(17), 9410 – 9464. DOI: https://doi.org/10.1021/acs.chemrev.5b00138.

29. Cramer, N., Seiser, T. (2011). β-Carbon Elimination from Cyclobutanols: A Clean Access to Alkylrhodium Intermediates Bearing a Quaternary Stereogenic Center, *Synlett*, *4*, 449 – 460. DOI: https://doi.org/10.1055/s-0030-1259536.

30. Nakao, Y., Dong, G., Ed. "Catalytic C–CN Bond Activation." *C-C Bond Activation*, Springer, Heidelberg, NY, 2014, pp. 33–58. DOI: https://doi.org/10.1007/978-3-642-55055-3.

31. Li H., Li Y., Zhang X. S., Chen K., Wang X., Shi Z. J. (2011) Pyridinyl directed alkenylation with olefins via Rh(III)-catalyzed C–C bond cleavage of secondary arylmethanols, *J. Am. Chem. Soc.*, *133*(39), 15244 – 15247. DOI: https://doi.org/10.1021/ja205228y.

32. Rodriguez, N., Goossen, L. J. (2011). Decarboxylative coupling reactions: a modern strategy for C–C-bond formation, *Chem. Soc. Rev.*, *40*(10), 5030 − 5048. DOI: https://doi.org/10.1039/C1CS15093F.

33. Nogi, K., Yorimitsu, H. (2021). Carbon–Carbon Bond Cleavage at Allylic Positions: Retro-Allylation and Deallylation, *Chem. Rev.*, *121*(1), 345 – 364. DOI: https://doi.org/10.1021/acs.chemrev.0c00157.

34. Garcia, J. J., Arevalo, A., Brunkan, N. M., Jones, W. D. (2004). Cleavage of Carbon−Carbon Bonds in Alkyl Cyanides Using Nickel(0), *Organometallics*, *23*(16), 3997 – 4002. DOI: https://doi.org/10.1021/om049700t.

35. Brunkan, N. M., Brestensky, D. M., Jones, W. D. (2004) Kinetics, Thermodynamics, and Effect of BPh_3 on Competitive C−C and C−H Bond Activation Reactions in the

Interconversion of Allyl Cyanide by [Ni(dippe)], *J. Am. Chem. Soc.*, *126*(11), 3627 – 3641. DOI: https://doi.org/10.1021/ja037002e.

36. Tolman, C. A., Seidel, W. C., Druliner, J. D., Domaille, P. J. (1984) Catalytic hydrocyanation of olefins by nickel(0) phosphite complexes - effects of Lewis acids, *Organometallics*, *3*(1), 33 – 38. DOI: https://doi.org/10.1021/om00079a008.

37. Li, T., Jones, W. D. (2011). DFT Calculations of the Isomerization of 2-Methyl-3-butenenitrile by [Ni(bisphosphine)] in Relation to the DuPont Adiponitrile Process, *Organometallics*, *30*(3), 547 – 555. DOI: https://doi.org/10.1021/om100907y.

38. Garcia, J. J., Brunkan, N. M., Jones, W. D. (2002). Cleavage of Carbon−Carbon Bonds in Aromatic Nitriles Using Nickel(0), *J. Am. Chem. Soc.*, *124*(32), 9547 – 9555. DOI: https://doi.org/10.1021/ja0204933.

39. Munjanja, L., Torres-López, C., Brennessel, W. W., Jones, W. D. (2016). C–CN Bond Cleavage Using Palladium Supported by a Dippe Ligand, *Organometallic*, *35*(11), 2010 – 2013. DOI: https://doi.org/10.1021/acs.organomet.6b00304.

40. Swartz B. D., Brennessel W. W., Jones W. D. (2011). C–CN vs C–H cleavage of benzonitrile using $[(dippe)PtH]_2$, *Organometallics*, *30*(6), 1523 – 1529. DOI: https://doi.org/10.1021/om101069j.

41. Macromodel, Release 2021-1, Schrödinger, LLC, New York, NY, 2021.

42. Chen, I. J., Foloppe, N. (2013). Tackling the conformational sampling of larger flexible compounds and macrocycles in pharmacology and drug discovery, *21*(24), 7898 – 7920. DOI: https://doi.org/10.1016/j.bmc.2013.10.003.

43. Jorgensen, W. L., Thomas, L. L. J. (2008). Perspective on Free-Energy Perturbation Calculations for Chemical Equilibria, *Chem. Theory Comput.*, *4*(6), 869–876. DOI: https://doi.org/10.1021/ct800011m.

44. Engel, Thomas, et al. "Appendix B." *Physical Chemistry,* Pearson, Boston, MA, 2013, pp. 1043.

45. Ponder, J. W., Richards, F. M. (1987). An efficient newton-like method for molecular mechanics energy minimization of large molecules, *J. Comp. Chem.*, *8*, 1016 – 1024. DOI: https://doi.org/10.1002/jcc.540080710.

46. Gallegos, D. C. (2021) *Investigation of the C–CN Bond Activation of Fluorinated Benzonitriles with [Ni(dmpe)] and DFT Benchmarking study with [Ni(dippe)]* [Unpublished Masters Thesis]. University of Texas Rio Grande Valley.

47. GaussView, Version 6, Dennington, Roy; Keith, Todd A.; Millam, John M. Semichem Inc., Shawnee Mission, KS, **2016**.

48. Becke, A. D. (1993). Density-functional thermochemistry. III. The role of exact exchange, *J. Chem. Phys*., *98*, 5648 – 5652. DOI: https://doi.org/10.1063/1.464913.

49. Grimme, S., Antony, J., Ehrlich, S., Krieg, H. (2010). A consistent and accurate ab initio parametrization of density functional dispersion correction (DFT-D) for the 94 elements H-Pu, *J. Chem. Phys*, *132*, 154104. DOI: https://doi.org/10.1063/1.3382344.

50. Ehlers, A.W.; Bohme, M.; Dapprich, S., Gobbi A., et. al. (1993)**.** A set of f-polarization functions for pseudo-potential basis sets of the transition metals Sc–Cu, Y–Ag and La–Au, *Chem Phys. Lett.*, *208*, 111 – 114. DOI: https://doi.org/10.1016/0009-2614(93)80086-5.

51. Hollwarth, A., Bohme, M., Dapprich, S., Ehlers, A.W., et. al. (1993). A set of d-polarization functions for pseudo-potential basis sets of the main group elements Al–Bi and f-type polarization functions for Zn, Cd, Hg, *Chem. Phys. Lett.*, *208*, 237 – 240. DOI: https://doi.org/10.1016/0009-2614(93)89068-S.

52. Ehnbom, A., Ghosh, S. K., Lewis, K. G., Gladysz J. A. (2016). Octahedral Werner complexes with substituted ethylenediamine ligands: a stereochemical primer for a historic series of compounds now emerging as a modern family of catalysts, *Chem. Soc. Rev.*, *45*, 6799 – 6811. DOI: https://doi.org/10.1039/c6cs00604c.

APPENDIX

APPENDIX

Table 6: Solvation energy and thermodynamic corrections for the 244 optimized unique conformers using B3LYP functional.

File Name	E/au	ZPE/au	H/au	T.S/au	T.qh-S/au	G(T)/au	qh-G(T)/au	ΔG (kcal/mol)
Nidippe_1	-736.928655	0.438186	-736.464559	0.079788	0.07585	-736.544348	-736.540409	0
Nidippe_100	-736.924191	0.438598	-736.459958	0.078851	0.075251	-736.53881	-736.535209	3.47515038
Nidippe_101	-736.923687	0.438743	-736.459355	0.078442	0.075058	-736.537797	-736.534413	4.11081801
Nidippe_102	-736.923659	0.438551	-736.459419	0.078926	0.075347	-736.538345	-736.534766	3.76694253
Nidippe_103	-736.921814	0.439272	-736.45718	0.077287	0.074381	-736.534467	-736.531561	6.20042631
Nidippe_104	-736.921813	0.439018	-736.457293	0.077987	0.074736	-736.53528	-736.532029	5.69026068
Nidippe_105	-736.921954	0.438571	-736.457591	0.079444	0.075626	-736.537035	-736.533217	4.58898063
Nidippe_106	-736.921954	0.438743	-736.457469	0.079213	0.075492	-736.536682	-736.532961	4.81049166
Nidippe_107	-736.923565	0.438813	-736.459062	0.079375	0.075496	-736.538438	-736.534558	3.7085841
Nidippe_108	-736.923592	0.438807	-736.459153	0.078598	0.075178	-736.537751	-736.534331	4.13968347
Nidippe_109	-736.920638	0.438713	-736.456265	0.07841	0.075214	-736.534676	-736.531479	6.06927672
Nidippe_10	-736.926578	0.439008	-736.462139	0.077661	0.074624	-736.5398	-736.536763	2.85391548
Nidippe_11	-736.926551	0.438403	-736.462317	0.079337	0.075663	-736.541654	-736.53798	1.69051194
Nidippe_110	-736.920665	0.438972	-736.456126	0.077931	0.074951	-736.534056	-736.531076	6.45833292
Nidippe_111	-736.923263	0.438714	-736.458841	0.078715	0.075258	-736.537556	-736.534099	4.26204792
Nidippe_112	-736.923283	0.438487	-736.458981	0.079225	0.075553	-736.538206	-736.534534	3.85416642
Nidippe_113	-736.923768	0.438924	-736.459379	0.078055	0.074693	-736.537433	-736.534072	4.33923165
Nidippe_114	-736.92376	0.438891	-736.459377	0.078413	0.074833	-736.53779	-736.53421	4.11521058
Nidippe_115	-736.921414	0.438649	-736.457037	0.079146	0.075451	-736.536183	-736.532488	5.12361915
Nidippe_116	-736.921445	0.438807	-736.456946	0.078974	0.075317	-736.53592	-736.532263	5.28865428
Nidippe_117	-736.925074	0.438769	-736.460699	0.078474	0.075025	-736.539173	-736.535724	3.24736425
Nidippe_118	-736.925064	0.438539	-736.460861	0.078566	0.075123	-736.539428	-736.535984	3.0873492
Nidippe_119	-736.92253	0.438883	-736.458065	0.078796	0.075317	-736.536861	-736.533382	4.69816737
Nidippe_12	-736.926574	0.43846	-736.462317	0.07917	0.075553	-736.541487	-736.53787	1.79530611
Nidippe_120	-736.922451	0.440299	-736.45719	0.075619	0.07352	-736.532809	-736.53071	7.24083789
Nidippe_121	-736.923487	0.438819	-736.459155	0.077834	0.074814	-736.536989	-736.53397	4.61784609
Nidippe_122	-736.923489	0.438693	-736.459204	0.078332	0.075036	-736.537536	-736.53424	4.27459812
Nidippe_122	-736.923489	0.438693	-736.459204	0.078332	0.075036	-736.537536	-736.53424	4.27459812
Nidippe_123	-736.922387	0.439032	-736.458754	0.075393	0.072839	-736.534146	-736.531592	6.40185702
Nidippe_124	-736.922389	0.439021	-736.45784	0.078717	0.075099	-736.536556	-736.532939	4.88955792
Nidippe_125	-736.921993	0.439068	-736.457424	0.077744	0.074762	-736.535168	-736.532186	5.7605418
Nidippe_126	-736.921986	0.439073	-736.457417	0.077742	0.074747	-736.535159	-736.532164	5.76618939
Nidippe_127	-736.922864	0.438754	-736.458513	0.078466	0.075108	-736.536979	-736.533621	4.62412119
Nidippe_128	-736.922846	0.438718	-736.458524	0.078477	0.075098	-736.537001	-736.533622	4.61031597
Nidippe_129	-736.922926	0.440493	-736.457578	0.075697	0.073237	-736.533275	-736.530815	6.94841823
Nidippe_13	-736.92655	0.438399	-736.462313	0.079602	0.075786	-736.541915	-736.538099	1.52673183
Nidippe_130	-736.922971	0.439184	-736.458438	0.077584	0.074428	-736.536021	-736.532866	5.22527577
Nidippe_131	-736.922533	0.43852	-736.458301	0.078788	0.075257	-736.537089	-736.533558	4.55509509
Nidippe_132	-736.922535	0.438642	-736.458247	0.078526	0.07513	-736.536773	-736.533376	4.75338825

Table 6, cont.

Nidippe_133	-736.924099	0.438579	-736.459765	0.079335	0.075553	-736.5391	-736.535318	3.29317248
Nidippe_134	-736.924132	0.438756	-736.459669	0.078963	0.075345	-736.538632	-736.535014	3.58684716
Nidippe_135	-736.921426	0.439107	-736.456904	0.077745	0.074639	-736.534648	-736.531543	6.086847
Nidippe_136	-736.921413	0.439151	-736.456849	0.077791	0.074647	-736.53464	-736.531496	6.09186708
Nidippe_137	-736.922168	0.43855	-736.45797	0.079281	0.075261	-736.537251	-736.533231	4.45343847
Nidippe_138	-736.922179	0.438621	-736.457953	0.079099	0.075187	-736.537051	-736.53314	4.57894047
Nidippe_139	-736.921439	0.438886	-736.457077	0.078309	0.074811	-736.535386	-736.531887	5.62374462
Nidippe_14	-736.926572	0.438435	-736.462324	0.079338	0.075626	-736.541662	-736.53795	1.68549186
Nidippe_140	-736.92145	0.439027	-736.457015	0.077862	0.07461	-736.534877	-736.531624	5.94314721
Nidippe_141	-736.922852	0.438819	-736.458384	0.079096	0.075337	-736.53748	-736.533721	4.30973868
Nidippe_142	-736.922861	0.439052	-736.458354	0.077497	0.074654	-736.535851	-736.533008	5.33195247
Nidippe_143	-736.924083	0.438645	-736.459835	0.078558	0.075075	-736.538393	-736.53491	3.73682205
Nidippe_144	-736.919487	0.438911	-736.454974	0.078934	0.075213	-736.533908	-736.530188	6.5512044
Nidippe_145	-736.919482	0.438907	-736.454982	0.07884	0.075182	-736.533823	-736.530165	6.60454275
Nidippe_146	-736.920328	0.438814	-736.455864	0.078371	0.075146	-736.534236	-736.53101	6.34538112
Nidippe_147	-736.920282	0.438568	-736.455939	0.07914	0.075543	-736.535079	-736.531482	5.81639019
Nidippe_148	-736.922227	0.43872	-736.457808	0.078953	0.075401	-736.536761	-736.53321	4.76091837
Nidippe_149	-736.922228	0.438729	-736.457818	0.07893	0.075412	-736.536748	-736.53323	4.769076
Nidippe_15	-736.928186	0.43856	-736.463903	0.078867	0.075377	-736.542771	-736.53928	0.98958327
Nidippe_150	-736.921957	0.438688	-736.457501	0.079363	0.075559	-736.536865	-736.533061	4.69565733
Nidippe_151	-736.921951	0.438574	-736.457573	0.079602	0.075695	-736.537175	-736.533268	4.50112923
Nidippe_152	-736.92181	0.439093	-736.457246	0.077857	0.074662	-736.535103	-736.531908	5.80132995
Nidippe_153	-736.921805	0.439108	-736.457239	0.07788	0.074674	-736.535118	-736.531913	5.7919173
Nidippe_154	-736.921171	0.438642	-736.456882	0.079141	0.075248	-736.536024	-736.53213	5.22339324
Nidippe_155	-736.92474	0.438151	-736.460714	0.079992	0.075845	-736.540706	-736.53656	2.28539142
Nidippe_156	-736.920644	0.43882	-736.456191	0.078405	0.075204	-736.534596	-736.531395	6.11947752
Nidippe_157	-736.920661	0.438722	-736.456276	0.078501	0.075253	-736.534777	-736.53153	6.00589821
Nidippe_158	-736.9216	0.438908	-736.457101	0.078124	0.0751	-736.535225	-736.532202	5.72477373
Nidippe_159	-736.921603	0.438702	-736.457211	0.078859	0.075389	-736.536069	-736.5326	5.19515529
Nidippe_160	-736.920627	0.438272	-736.456602	0.07979	0.075585	-736.536392	-736.532187	4.99246956
Nidippe_161	-736.920636	0.43839	-736.456553	0.079305	0.07536	-736.535859	-736.531913	5.32693239
Nidippe_162	-736.920512	0.439037	-736.455998	0.078051	0.074726	-736.534049	-736.530724	6.46272549
Nidippe_163	-736.920508	0.438979	-736.456015	0.078177	0.074789	-736.534192	-736.530804	6.37299156
Nidippe_164	-736.920513	0.43904	-736.455983	0.078053	0.07476	-736.534035	-736.530743	6.47151063
Nidippe_165	-736.9205	0.43888	-736.456035	0.078589	0.074989	-736.534623	-736.531023	6.10253475
Nidippe_166	-736.923641	0.438581	-736.459388	0.079074	0.075384	-736.538462	-736.534772	3.69352386
Nidippe_167	-736.923686	0.438627	-736.459416	0.07869	0.075194	-736.538106	-736.53461	3.91691742
Nidippe_168	-736.91988	0.438564	-736.455564	0.079136	0.075395	-736.534701	-736.530959	6.05358897
Nidippe_169	-736.919933	0.439096	-736.455295	0.078501	0.074916	-736.533796	-736.530211	6.62148552
Nidippe_16	-736.926157	0.438623	-736.461831	0.079001	0.075463	-736.540832	-736.537295	2.20632516
Nidippe_17	-736.92616	0.438574	-736.461877	0.07884	0.075433	-736.540717	-736.53731	2.27848881
Nidippe_170	-736.921923	0.438879	-736.457515	0.078346	0.074834	-736.535861	-736.532349	5.32567737
Nidippe_171	-736.921907	0.438907	-736.457481	0.078283	0.0748	-736.535763	-736.53228	5.38717335
Nidippe_172	-736.919481	0.43885	-736.45509	0.078312	0.074942	-736.533402	-736.530032	6.86872446
Nidippe_173	-736.919464	0.439059	-736.454977	0.077758	0.074631	-736.532735	-736.529608	7.28727363
Nidippe_174	-736.921799	0.439103	-736.457222	0.077925	0.074688	-736.535147	-736.53191	5.77371951
Nidippe_175	-736.921828	0.439396	-736.457106	0.077268	0.074302	-736.534374	-736.531408	6.25878474
Nidippe_176	-736.921096	0.438532	-736.456924	0.079027	0.075237	-736.53595	-736.532161	5.26982898
Nidippe_177	-736.9211	0.438547	-736.456914	0.079029	0.075235	-736.535943	-736.532148	5.27422155
Nidippe_178	-736.918951	0.438979	-736.454418	0.078521	0.074956	-736.532939	-736.529374	7.15926159
Nidippe_179	-736.918949	0.438897	-736.454476	0.078564	0.074997	-736.533039	-736.529472	7.09651059
Nidippe_18	-736.926996	0.438493	-736.462739	0.079041	0.075514	-736.54178	-736.538253	1.61144568

Table 6, cont.

Nidippe_180	-736.92041	0.438684	-736.45613	0.07864	0.075059	-736.534771	-736.53119	6.00966327
Nidippe_181	-736.920415	0.43873	-736.456091	0.078859	0.075114	-736.53495	-736.531205	5.89733898
Nidippe_183	-736.921613	0.438839	-736.457133	0.078677	0.075229	-736.53581	-736.532363	5.35768038
Nidippe_184	-736.921828	0.438693	-736.457568	0.07872	0.074995	-736.536287	-736.532563	5.05835811
Nidippe_185	-736.92182	0.438684	-736.457562	0.078764	0.075028	-736.536326	-736.53259	5.03388522
Nidippe_186	-736.920735	0.439292	-736.456049	0.077637	0.074534	-736.533686	-736.530583	6.69051162
Nidippe_187	-736.920681	0.439025	-736.45617	0.077947	0.074745	-736.534117	-736.530915	6.42005481
Nidippe_188	-736.919261	0.438982	-736.454667	0.078711	0.075133	-736.533378	-736.5298	6.8837847
Nidippe_189	-736.919257	0.438866	-736.454708	0.079015	0.075304	-736.533723	-736.530012	6.66729375
Nidippe_19	-736.926995	0.438554	-736.462692	0.079248	0.075587	-736.54194	-736.538278	1.51104408
Nidippe_190	-736.920672	0.438858	-736.456222	0.078172	0.075084	-736.534394	-736.531306	6.24623454
Nidippe_191	-736.920634	0.43873	-736.456227	0.078612	0.075306	-736.534839	-736.531533	5.96699259
Nidippe_192	-736.921325	0.438447	-736.457163	0.079521	0.075455	-736.536684	-736.532618	4.80923664
Nidippe_193	-736.920582	0.438795	-736.456274	0.078128	0.074786	-736.534401	-736.531059	6.24184197
Nidippe_194	-736.918852	0.438965	-736.454373	0.078151	0.074854	-736.532525	-736.529227	7.41905073
Nidippe_195	-736.918881	0.439003	-736.454368	0.07814	0.074847	-736.532509	-736.529215	7.42909089
Nidippe_196	-736.918323	0.439124	-736.453665	0.078283	0.07495	-736.531948	-736.528615	7.781124
Nidippe_197	-736.918332	0.439191	-736.453626	0.078296	0.074929	-736.531922	-736.528554	7.79743926
Nidippe_198	-736.919725	0.43884	-736.455307	0.078265	0.074934	-736.533573	-736.530241	6.76142025
Nidippe_199	-736.919716	0.439016	-736.455186	0.078298	0.074878	-736.533483	-736.530064	6.81789615
Nidippe_2	-736.928658	0.438387	-736.464412	0.07968	0.075739	-736.544092	-736.540151	0.16064256
Nidippe_20	-736.927145	0.438836	-736.462754	0.078253	0.074902	-736.541007	-736.537657	2.09651091
Nidippe_200	-736.917326	0.438852	-736.452885	0.078378	0.075099	-736.531263	-736.527983	8.21096835
Nidippe_201	-736.917369	0.439089	-736.452794	0.077843	0.074783	-736.530636	-736.527576	8.60441712
Nidippe_202	-736.923468	0.438584	-736.459263	0.07835	0.075107	-736.537613	-736.534369	4.22627985
Nidippe_203	-736.923489	0.438768	-736.45917	0.077998	0.074917	-736.537168	-736.534086	4.5055218
Nidippe_205	-736.918996	0.438788	-736.45463	0.078529	0.075086	-736.533158	-736.529715	7.0218369
Nidippe_206	-736.918658	0.43912	-736.454062	0.078087	0.074792	-736.532148	-736.528853	7.655622
Nidippe_207	-736.918696	0.439303	-736.454	0.077649	0.07455	-736.531649	-736.528551	7.96874949
Nidippe_208	-736.918648	0.438975	-736.45413	0.078309	0.074932	-736.532439	-736.529061	7.47301659
Nidippe_209	-736.918665	0.439013	-736.454136	0.078443	0.07494	-736.532579	-736.529076	7.38516519
Nidippe_21	-736.927133	0.438859	-736.462745	0.078034	0.074804	-736.54078	-736.537549	2.23895568
Nidippe_210	-736.91815	0.439011	-736.453604	0.07832	0.074941	-736.531924	-736.528545	7.79618424
Nidippe_211	-736.918155	0.438981	-736.453634	0.078278	0.074941	-736.531912	-736.528575	7.80371436
Nidippe_212	-736.921221	0.438633	-736.456953	0.078856	0.075123	-736.535809	-736.532076	5.35830789
Nidippe_213	-736.92124	0.438851	-736.456858	0.078457	0.074858	-736.535315	-736.531716	5.66829783
Nidippe_214	-736.920632	0.438396	-736.456539	0.079228	0.075361	-736.535767	-736.5319	5.38466331
Nidippe_215	-736.92061	0.438284	-736.456601	0.07951	0.075517	-736.536111	-736.532118	5.16879987
Nidippe_216	-736.921098	0.4386	-736.456897	0.07883	0.075118	-736.535727	-736.532015	5.40976371
Nidippe_217	-736.92346	0.438616	-736.459232	0.078334	0.075077	-736.537567	-736.53431	4.25514531
Nidippe_218	-736.918669	0.439107	-736.454002	0.078165	0.074914	-736.532167	-736.528916	7.64369931
Nidippe_219	-736.920509	0.439058	-736.455987	0.077994	0.074698	-736.533981	-736.530685	6.50539617
Nidippe_22	-736.925076	0.438087	-736.461986	0.076484	0.073891	-736.538469	-736.535877	3.68913129
Nidippe_220	-736.918646	0.438923	-736.454085	0.078664	0.075139	-736.53275	-736.529224	7.27786098
Nidippe_221	-736.921258	0.438699	-736.456916	0.078404	0.07521	-736.53532	-736.532126	5.66516028
Nidippe_222	-736.921268	0.438605	-736.456991	0.078468	0.07528	-736.53546	-736.532272	5.57730888
Nidippe_223	-736.917668	0.43917	-736.452964	0.078063	0.074841	-736.531027	-736.527805	8.35906071
Nidippe_224	-736.917668	0.439228	-736.452939	0.078102	0.074794	-736.531041	-736.527734	8.35027557
Nidippe_225	-736.918182	0.438989	-736.453647	0.078335	0.074961	-736.531982	-736.528608	7.75978866
Nidippe_226	-736.918157	0.438698	-736.453788	0.078946	0.075329	-736.532733	-736.529117	7.28852865
Nidippe_227	-736.920704	0.438833	-736.456263	0.078931	0.075159	-736.535194	-736.531422	5.74422654
Nidippe_228	-736.920706	0.438841	-736.456276	0.078798	0.075092	-736.535075	-736.531369	5.81890023

Table 6, cont.

Nidippe_229	-736.919333	0.438718	-736.454949	0.079092	0.075286	-736.534041	-736.530235	6.46774557
Nidippe_23	-736.925115	0.438438	-736.460914	0.078943	0.075615	-736.539857	-736.536529	2.81814741
Nidippe_230	-736.919319	0.438572	-736.45503	0.079327	0.07543	-736.534357	-736.53046	6.26945241
Nidippe_231	-736.919728	0.438849	-736.455311	0.078205	0.074892	-736.533516	-736.530203	6.79718832
Nidippe_232	-736.919241	0.438789	-736.454821	0.078932	0.0752	-736.533753	-736.530021	6.64846845
Nidippe_233	-736.919266	0.438889	-736.454761	0.079121	0.075257	-736.533882	-736.530018	6.56751966
Nidippe_234	-736.91968	0.438814	-736.455283	0.078678	0.075086	-736.533961	-736.53037	6.51794637
Nidippe_235	-736.919678	0.438772	-736.455297	0.078923	0.075198	-736.53422	-736.530494	6.35542128
Nidippe_236	-736.918313	0.43866	-736.454006	0.07872	0.075171	-736.532726	-736.529178	7.29292122
Nidippe_237	-736.921094	0.438569	-736.456905	0.078991	0.07519	-736.535896	-736.532095	5.30371452
Nidippe_238	-736.921096	0.438655	-736.456852	0.078944	0.075162	-736.535795	-736.532013	5.36709303
Nidippe_239	-736.918678	0.439159	-736.454065	0.07803	0.074732	-736.532095	-736.528798	7.68888003
Nidippe_24	-736.925331	0.439405	-736.460699	0.076817	0.07406	-736.537516	-736.53476	4.28714832
Nidippe_240	-736.918691	0.43909	-736.454098	0.078315	0.074898	-736.532412	-736.528996	7.48995936
Nidippe_241	-736.918678	0.439095	-736.454106	0.078061	0.074777	-736.532166	-736.528883	7.64432682
Nidippe_242	-736.918677	0.439042	-736.454129	0.078223	0.074856	-736.532352	-736.528985	7.52760996
Nidippe_243	-736.917372	0.439074	-736.452799	0.07791	0.074843	-736.530709	-736.527642	8.55860889
Nidippe_244	-736.917352	0.439098	-736.452777	0.077721	0.074763	-736.530498	-736.52754	8.6910135
Nidippe_25	-736.9253	0.439204	-736.460777	0.07719	0.074296	-736.537967	-736.535074	4.00414131
Nidippe_26	-736.926574	0.438481	-736.462289	0.079327	0.075612	-736.541616	-736.537901	1.71435732
Nidippe_27	-736.927744	0.438695	-736.463454	0.078038	0.075041	-736.541493	-736.538495	1.79154105
Nidippe_28	-736.927754	0.438897	-736.463351	0.07772	0.07478	-736.541071	-736.538131	2.05635027
Nidippe_29	-736.928171	0.438397	-736.463991	0.079077	0.075513	-736.543068	-736.539504	0.8032128
Nidippe_3	-736.928185	0.43855	-736.463916	0.078696	0.075308	-736.542612	-736.539224	1.08935736
Nidippe_30	-736.924987	0.438793	-736.460614	0.078401	0.07502	-736.539015	-736.535634	3.34651083
Nidippe_31	-736.924987	0.438927	-736.460539	0.078138	0.074865	-736.538677	-736.535404	3.55860921
Nidippe_32	-736.926576	0.438998	-736.462149	0.077609	0.0746	-736.539758	-736.536749	2.8802709
Nidippe_33	-736.926606	0.439174	-736.462084	0.077282	0.074391	-736.539365	-736.536475	3.12688233
Nidippe_34	-736.8957	0.438957	-736.430956	0.079872	0.075909	-736.510828	-736.506865	21.0341352
Nidippe_35	-736.927149	0.438871	-736.462748	0.078062	0.074817	-736.54081	-736.537565	2.22013038
Nidippe_36	-736.926567	0.438782	-736.462258	0.07814	0.074895	-736.540398	-736.537153	2.4786645
Nidippe_37	-736.926579	0.438899	-736.462214	0.077787	0.074725	-736.540001	-736.536938	2.72778597
Nidippe_38	-736.924419	0.438509	-736.460081	0.07957	0.075727	-736.539651	-736.535808	2.94741447
Nidippe_39	-736.926148	0.438973	-736.461653	0.078154	0.075021	-736.539807	-736.536674	2.84952291
Nidippe_4	-736.928191	0.438364	-736.464042	0.079029	0.075507	-736.543072	-736.53955	0.80070276
Nidippe_40	-736.926578	0.438496	-736.462284	0.079261	0.075569	-736.541545	-736.537854	1.75891053
Nidippe_41	-736.926551	0.438426	-736.462304	0.07927	0.075629	-736.541574	-736.537933	1.74071274
Nidippe_42	-736.926557	0.438322	-736.46235	0.079816	0.07589	-736.542166	-736.53824	1.36922682
Nidippe_43	-736.926574	0.438463	-736.46231	0.079291	0.075603	-736.541601	-736.537913	1.72376997
Nidippe_44	-736.923392	0.438656	-736.459043	0.078964	0.075368	-736.538007	-736.534411	3.97904091
Nidippe_45	-736.9234	0.438675	-736.459055	0.078757	0.075279	-736.537812	-736.534334	4.10140536
Nidippe_46	-736.924758	0.438478	-736.460501	0.079207	0.075666	-736.539709	-736.536167	2.91101889
Nidippe_47	-736.924737	0.438272	-736.460623	0.079356	0.075794	-736.539979	-736.536416	2.74159119
Nidippe_48	-736.924978	0.438682	-736.460661	0.078673	0.075183	-736.539334	-736.535844	3.14633514
Nidippe_49	-736.924985	0.438884	-736.460552	0.078271	0.074934	-736.538823	-736.535486	3.46699275
Nidippe_5	-736.927733	0.438536	-736.463528	0.078638	0.075323	-736.542166	-736.538851	1.36922682
Nidippe_50	-736.925115	0.438395	-736.460939	0.079072	0.075678	-736.540011	-736.536617	2.72151087
Nidippe_51	-736.925094	0.438404	-736.460912	0.079262	0.075756	-736.540174	-736.536668	2.61922674
Nidippe_52	-736.925064	0.43848	-736.460874	0.07878	0.075249	-736.539654	-736.536124	2.94553194
Nidippe_53	-736.925069	0.438574	-736.46083	0.078542	0.075126	-736.539372	-736.535956	3.12248976
Nidippe_54	-736.926146	0.438569	-736.461865	0.078882	0.075434	-736.540747	-736.537299	2.25966351
Nidippe_55	-736.924933	0.43887	-736.460548	0.077986	0.074789	-736.538534	-736.535337	3.64834314

Table 6, cont.

Nidippe_56	-736.924898	0.438616	-736.460641	0.078562	0.075122	-736.539202	-736.535763	3.22916646
Nidippe_57	-736.921494	0.438757	-736.457082	0.07952	0.075392	-736.536602	-736.532473	4.86069246
Nidippe_58	-736.921484	0.438697	-736.457098	0.079585	0.07547	-736.536683	-736.532567	4.80986415
Nidippe_59	-736.926435	0.438457	-736.462257	0.078826	0.075486	-736.541082	-736.537743	2.04944766
Nidippe_6	-736.927744	0.438696	-736.463451	0.078085	0.075063	-736.541536	-736.538514	1.76455812
Nidippe_60	-736.926444	0.438589	-736.462174	0.078655	0.075367	-736.540828	-736.537541	2.2088352
Nidippe_61	-736.922998	0.438808	-736.458538	0.078954	0.075249	-736.537492	-736.533787	4.30220856
Nidippe_62	-736.922989	0.438702	-736.458623	0.078763	0.075223	-736.537386	-736.533846	4.36872462
Nidippe_63	-736.924422	0.438546	-736.460068	0.079396	0.075647	-736.539465	-736.535715	3.06413133
Nidippe_64	-736.924421	0.438642	-736.460047	0.078893	0.075457	-736.53894	-736.535504	3.39357408
Nidippe_65	-736.92347	0.438689	-736.459216	0.078121	0.074955	-736.537337	-736.534171	4.39947261
Nidippe_66	-736.923476	0.438718	-736.459205	0.078025	0.074904	-736.537229	-736.534108	4.46724369
Nidippe_67	-736.923401	0.438586	-736.459102	0.079014	0.075408	-736.538116	-736.534509	3.91064232
Nidippe_68	-736.923388	0.438601	-736.459089	0.078943	0.075385	-736.538032	-736.534474	3.96335316
Nidippe_7	-736.927146	0.438835	-736.462763	0.078146	0.074867	-736.540909	-736.53763	2.15800689
Nidippe_70	-736.925304	0.438846	-736.460925	0.078257	0.074988	-736.539182	-736.535913	3.24171666
Nidippe_71	-736.923398	0.439049	-736.458942	0.077708	0.07455	-736.53665	-736.533492	4.83057198
Nidippe_72	-736.923418	0.439067	-736.458976	0.077458	0.074425	-736.536434	-736.533401	4.96611414
Nidippe_73	-736.925055	0.438556	-736.460806	0.078881	0.075249	-736.539687	-736.536055	2.92482411
Nidippe_74	-736.925078	0.438682	-736.46077	0.07834	0.07502	-736.539109	-736.53579	3.28752489
Nidippe_75	-736.924762	0.438299	-736.460648	0.079598	0.075636	-736.540245	-736.536284	2.57467353
Nidippe_76	-736.924756	0.438255	-736.460689	0.079948	0.075751	-736.540636	-736.53644	2.32931712
Nidippe_77	-736.92288	0.438302	-736.458793	0.079417	0.075646	-736.538209	-736.534439	3.85228389
Nidippe_78	-736.922914	0.438508	-736.458713	0.078964	0.075369	-736.537677	-736.534082	4.18611921
Nidippe_79	-736.923097	0.438623	-736.458814	0.078756	0.075223	-736.53757	-736.534037	4.25326278
Nidippe_8	-736.927132	0.438803	-736.462769	0.078184	0.074893	-736.540953	-736.537663	2.13039645
Nidippe_80	-736.923092	0.438578	-736.458853	0.078802	0.075251	-736.537655	-736.534104	4.19992443
Nidippe_81	-736.926549	0.438357	-736.462345	0.079383	0.075679	-736.541728	-736.538023	1.6440762
Nidippe_82	-736.923153	0.438842	-736.458688	0.078499	0.075145	-736.537187	-736.533833	4.49359911
Nidippe_83	-736.924542	0.438814	-736.460158	0.078605	0.075096	-736.538764	-736.535254	3.50401584
Nidippe_84	-736.924585	0.439045	-736.460079	0.077821	0.074678	-736.537899	-736.534756	4.04681199
Nidippe_85	-736.924499	0.438434	-736.460319	0.07914	0.075414	-736.539459	-736.535733	3.06789639
Nidippe_86	-736.924515	0.438511	-736.460282	0.079095	0.075369	-736.539378	-736.535652	3.1187247
Nidippe_87	-736.922529	0.438838	-736.458098	0.07859	0.075211	-736.536688	-736.53331	4.8067266
Nidippe_88	-736.92253	0.438904	-736.458059	0.078523	0.075179	-736.536582	-736.533238	4.87324266
Nidippe_89	-736.921909	0.438878	-736.457493	0.078325	0.074831	-736.535819	-736.532324	5.35203279
Nidippe_9	-736.926567	0.43881	-736.462247	0.078059	0.07484	-736.540306	-736.537087	2.53639542
Nidippe_90	-736.921921	0.438826	-736.457551	0.078368	0.074869	-736.53592	-736.53242	5.28865428
Nidippe_91	-736.921503	0.438717	-736.45712	0.079599	0.075443	-736.53672	-736.532563	4.78664628
Nidippe_92	-736.921485	0.438689	-736.457096	0.079731	0.075576	-736.536827	-736.532672	4.71950271
Nidippe_93	-736.922396	0.439099	-736.45781	0.078375	0.074938	-736.536185	-736.532748	5.12236413
Nidippe_94	-736.922404	0.439072	-736.457851	0.078211	0.074814	-736.536062	-736.532665	5.19954786
Nidippe_95	-736.923343	0.438655	-736.459013	0.079041	0.07531	-736.538054	-736.534323	3.94954794
Nidippe_96	-736.923309	0.438187	-736.459253	0.080088	0.075903	-736.539341	-736.535156	3.14194257
Nidippe_97	-736.923409	0.439097	-736.458931	0.077565	0.074471	-736.536496	-736.533402	4.92720852
Nidippe_98	-736.923396	0.439023	-736.458991	0.077446	0.074455	-736.536437	-736.533446	4.96423161
Nidippe_99	-736.924185	0.438487	-736.460017	0.079122	0.075374	-736.539139	-736.535391	3.26869959

Table 7: Dihedral angles of the 244 optimized structures, along with their backbone, gauche (-), gauche (+), and anti-periplanar configurations. Separated by their backbone configuration.

File Name	1,2,8,9	1,2,18,19	1,3,34,35	1,3,44,45	2,24,27,3		Name	Back bone
Nidippe_92.log:	-163.9976	-158.0936	-163.7787	-157.879	-42.1329	AAAA	aaaa	δ
Nidippe_58.log:	-163.785	-158.4068	-163.8532	-157.6896	-42.1533	-		δ
Nidippe_67.log:	-164.2465	-159.5767	158.0479	-56.956	-46.1217	AAAB	aaag-	δ
Nidippe_1.log:	-82.987	-158.0739	-82.7765	-157.1226	-39.8393	BABA	g-ag-a	δ
Nidippe_155.log:	-81.7261	-157.7297	-105.152	-47.3577	-45.4472	BABB	g-ag-g-	δ
Nidippe_133.log:	-81.6991	-158.2816	-82.3484	-13.3302	-45.5459	BABB	g-ag-g-	δ
Nidippe_40.log:	-82.3032	-156.6274	55.8908	-160.41	-39.0315	BACA	g-ag+a	δ
Nidippe_12.log:	-82.2423	-156.6602	55.9202	-160.3051	-38.9269	-		δ
Nidippe_19.log:	-81.477	-158.0776	159.0336	-56.8965	-44.7898	BAAB	g-aag-	δ
Nidippe_35.log:	-80.6753	-157.0774	145.2287	176.6498	-40.4045	BAAA	g-aaa	δ
Nidippe_7.log:	-80.7288	-157.1313	145.1496	176.6757	-40.3994	-		δ
Nidippe_20.log:	-80.7329	-157.2894	144.9968	176.6779	-40.4581	-		δ
Nidippe_75.log:	-104.7725	-47.7663	-81.5327	-157.9186	-45.2185	BBBA	g-g-g-a	δ
Nidippe_214.log:	-105.8283	-49.0788	-105.8546	-49.1687	-50.9459	BBBB	g-g-g-g-	δ
Nidippe_161.log:	-105.8131	-48.6447	-105.6221	-48.9114	-50.9411	-		δ
Nidippe_189.log:	-82.4508	-13.7096	-82.0302	-13.5528	-51.8658	BBBB	g-g-g-g-	δ
Nidippe_106.log:	-81.8453	-13.6509	56.0221	-161.1071	-45.6971	BBCA	g-g-g+a	δ
Nidippe_150.log:	-82.2836	-13.8877	56.0681	-160.9277	-45.5371	-		δ
Nidippe_196.log:	-82.3109	-13.406	30.4873	-54.2278	-50.1193	BBCB	g-g-g+g-	δ
Nidippe_224.log:	-82.2929	-13.1971	54.616	-19.2548	-52.1467	BBCB	g-g-g+g-	δ
Nidippe_216.log:	-106.1725	-48.7559	48.0108	115.7006	-50.7033	BBCC	g-g-g+g+	δ
Nidippe_237.log:	-105.5533	-49.0828	48.0359	115.9723	-50.4395	-		δ
Nidippe_219.log:	-82.6235	-13.0725	48.2374	116.2946	-51.0182	BBCC	g-g-g+g+	δ
Nidippe_162.log:	-82.4983	-12.9203	48.5196	116.6501	-50.8781	-		δ
Nidippe_93.log:	-80.4866	-13.2229	145.5662	177.2053	-46.5142	BBAA	g-g-aa	δ
Nidippe_124.log:	-81.0691	-13.2293	145.7992	177.0824	-46.3246	-		δ
Nidippe_107.log:	-82.1667	-13.1299	152.0796	74.9051	-46.4012	BBAC	g-g-ag+	δ
Nidippe_148.log:	-81.8401	-13.7214	158.915	-57.5783	-50.4027	BBAB	g-g-ag-	δ
Nidippe_95.log:	-81.447	118.4365	56.4472	-160.6397	-44.3682	BCCA	g-g+g+a	δ
Nidippe_170.log:	-81.4792	118.8537	-162.4818	-160.3114	-46.5128	BCAA	g-g+aa	δ
Nidippe_90.log:	-81.4801	118.6584	-162.7826	-159.8447	-46.5417	-		δ
Nidippe_132.log:	-107.1367	78.095	55.6371	-159.082	-41.6423	BCCA	g-g+g+a	δ
Nidippe_86.log:	-107.6223	75.6961	-82.672	-155.413	-42.109	BCBA	g-g+g-a	δ
Nidippe_192.log:	-81.6111	118.4373	-106.078	-48.5024	-50.4832	BCBB	g-g+g-g-	δ

Table 7, cont.

Nidippe_228.log:	-80.5894	117.6805	-82.486	-13.4494	-51.253	BCBB	g-g+g-g-	δ
Nidippe_234.log:	-80.5512	118.1503	30.2806	-54.1915	-49.6769	BCCB	g-g+g+g-	δ
Nidippe_178.log:	-81.007	117.6195	54.0622	-19.3592	-51.6793	BCCB	g-g+g+g-	δ
Nidippe_210.log:	-107.7386	75.128	53.7593	-18.8945	-48.6869	BCCB	g-g+g+g-	δ
Nidippe_225.log:	-107.7594	75.1187	53.762	-18.8902	-48.6543	-		δ
Nidippe_167.log:	-80.2678	117.2514	157.9403	-57.6054	-50.1693	BCAB	g-g+ag-	δ
Nidippe_101.log:	-80.5644	118.1684	158.3744	-57.3738	-49.7143	-		δ
Nidippe_128.log:	-105.5513	74.8357	158.2382	-56.7733	-46.7728	BCAB	g-g+ag-	δ
Nidippe_181.log:	-106.7151	76.7523	-106.8619	76.9043	-44.3272	BCBC	g-g+g-g+	δ
Nidippe_138.log:	-80.8503	117.9885	-81.0167	118.272	-50.6023	BCBC	g-g+g-g+	δ
Nidippe_212.log:	-107.9557	75.7058	-81.9156	118.3368	-47.5524	BCBC	g-g+g-g+	δ
Nidippe_56.log:	-81.776	120.5314	151.6039	76.9864	-45.587	BAAC	g-aag+	δ
Nidippe_185.log:	-80.8817	118.4116	48.3251	116.3165	-50.3125	BCCC	g-g+g+g+	δ
Nidippe_114.log:	-80.5144	120.6714	146.203	176.8382	-45.127	BAAA	g-aaa	δ
Nidippe_129.log:	-108.2029	76.3667	145.4544	176.9298	-42.7824	BCAA	g-g+aa	δ
Nidippe_62.log:	55.5522	-159.352	-162.6811	-158.8116	-40.0932	CAAA	g+aaa	δ
Nidippe_42.log:	55.9576	-160.276	-82.059	-156.5732	-38.8426	CABA	g+ag-a	δ
Nidippe_13.log:	55.9437	-160.2584	-82.0464	-155.988	-38.9335	-		δ
Nidippe_38.log:	56.1867	-159.7394	56.2267	-160.1377	-38.096	CACA	g+ag+a	δ
Nidippe_63.log:	56.0353	-159.8886	56.2568	-160.0529	-38.076	-		δ
Nidippe_47.log:	56.5289	-160.323	158.4559	-57.1272	-44.3202	CAAB	g+aag-	δ
Nidippe_31.log:	56.9504	-160.3119	145.5274	176.8888	-39.5353	CAAA	g+aaa	δ
Nidippe_49.log:	56.9787	-160.3227	145.4624	176.9091	-39.5564	-		δ
Nidippe_144.log:	30.0274	-53.7218	-164.7135	-159.0256	-45.6342	CBAA	g+g-aa	δ
Nidippe_82.log:	30.0792	-53.6485	-81.8278	-158.2701	-44.2315	CBBA	g+g-g-a	δ
Nidippe_205.log:	30.0009	-54.1558	-105.2707	-48.87	-49.8058	CBBB	g+g-g-g-	δ
Nidippe_194.log:	29.7725	-53.6827	-106.4849	74.0777	-46.5018	CBBC	g+g-g-g+	δ
Nidippe_201.log:	30.0884	-54.1314	30.3375	-54.1156	-49.0129	CBCB	g+g-g+g-	δ
Nidippe_244.log:	30.2462	-54.2502	30.3848	-54.2111	-48.9322	-		δ
Nidippe_208.log:	53.9394	-19.4701	48.4152	116.4144	-51.3248	CBCC	g+g-g+g+	δ
Nidippe_241.log:	54.032	-19.391	48.514	116.6754	-51.2525	-		δ
Nidippe_146.log:	54.5531	-19.6771	55.5639	-160.5985	-46.0299	CBCA	g+g-g+a	δ
Nidippe_156.log:	54.8567	-19.3237	158.4647	-58.6085	-50.8259	CBAB	g+g-ag-	δ
Nidippe_109.log:	54.8157	-19.3394	158.3977	-58.1371	-50.9428	-		δ
Nidippe_87.log:	30.1843	-53.4252	151.8133	74.8684	-45.0162	CBAC	g+g-ag+	δ
Nidippe_120.log	31.7755	-54.0788	151.2613	76.8294	-44.7611	-		δ
Nidippe_136.log:	30.7774	-54.595	144.991	177.4829	-45.2756	CBAA	g+g-aa	δ

Table 7, cont.

Nidippe_169.log:	24.2075	81.9331	-162.8737	-159.889	-43.6433	CCAA	g+g+aa	δ
Nidippe_112.log:	25.3221	77.8311	-83.5193	-157.7775	-42.1194	CCBA	g+g+g-a	δ
Nidippe_52.log:	47.6913	118.8573	-82.0115	-157.1768	-44.4481	CCBA	g+g+g-a	δ
Nidippe_74.log:	47.6257	118.9893	-81.8619	-157.0992	-44.3136	-		δ
Nidippe_118.log:	47.8395	118.132	-81.7426	-156.9124	-44.5303	-		δ
Nidippe_177.log:	47.9174	116.7273	-105.5944	-49.0295	-50.567	CCBB	g+g+g-g-	δ
Nidippe_230.log:	24.6185	79.8543	-104.7663	-48.6612	-47.63	CCBB	g+g+g-g-	δ
Nidippe_164.log:	48.3252	116.3568	-82.329	-12.904	-50.9881	CCBB	g+g+g-g-	δ
Nidippe_220.log:	25.2097	78.0256	-82.9324	-12.8428	-47.9698	CCBB	g+g+g-g-	δ
Nidippe_232.log:	24.5069	82.3511	-107.0915	75.4876	-44.4859	CCBC	g+g+g-g+	δ
Nidippe_115.log:	24.4713	83.1098	55.8185	-160.4901	-41.9008	CCCA	g+g+g+a	δ
Nidippe_80.log:	48.2014	115.4247	55.4553	-160.4358	-44.6022	CCCA	g+g+g+a	δ
Nidippe_172.log:	48.2223	116.4389	30.3868	-54.9517	-49.5383	CCCB	g+g+g+g-	δ
Nidippe_239.log:	48.4168	116.0919	54.0615	-19.4331	-51.1472	CCCB	g+g+g+g-	δ
Nidippe_207.log:	48.5417	115.8807	53.987	-19.0714	-51.3653	-		δ
Nidippe_139.log:	48.226	116.0491	48.1078	115.9876	-49.9827	CCCC	g+g+g+g+	δ
Nidippe_231.log:	25.385	77.8546	47.88	115.9117	-47.0254	CCCC	g+g+g+g+	δ
Nidippe_198.log:	25.3912	77.6228	47.7386	116.0537	-46.9556	-		δ
Nidippe_121.log:	48.8228	116.2357	158.4567	-58.0307	-49.7493	CCAB	g+g+ag-	δ
Nidippe_65.log:	48.6591	116.4838	157.889	-57.5743	-49.6187	-		δ
Nidippe_183.log:	25.3052	79.8157	158.2644	-57.3549	-47.1239	CCAB	g+g+ag-	δ
Nidippe_158.log:	25.2294	80.2003	157.9622	-57.1206	-47.0345	-		δ
Nidippe_84.log:	47.8553	118.6933	152.449	76.6997	-45.6242	CCAC	g+g+ag+	δ
Nidippe_141.log:	25.7472	78.2885	150.2581	78.9054	-43.248	CCAC	g+g+ag+	δ
Nidippe_153.log:	26.5021	76.9654	145.6255	176.8932	-42.4357	CCAA	g+g+aa	δ
Nidippe_174.log:	26.3271	77.0107	145.6009	177.0502	-42.4605	-		δ
Nidippe_103.log:	26.2573	77.3492	145.8011	177.0412	-42.3927	-		δ
Nidippe_97.log:	48.4617	118.4663	147.2315	176.5039	-45.2651	CCAA	g+g+aa	δ
Nidippe_71.log:	48.5112	119.014	147.1059	176.6509	-45.1269	-	g+g+aa	δ
Nidippe_45.log:	158.4421	-57.1262	-163.8014	-159.728	-46.339	ABAA	ag-aa	δ
Nidippe_77.log:	158.1731	-57.6799	-105.0056	-48.5958	-50.1751	ABBB	ag-g-g-	δ
Nidippe_221.log:	158.53	-57.5847	30.624	-54.0134	-49.2587	ABCB	ag-g+g-	δ
Nidippe_190.log:	158.6642	-58.4133	54.962	-19.3797	-50.8933	ABCB	ag-g+g-	δ
Nidippe_202.log:	158.2411	-57.9911	48.5146	116.0993	-49.6688	ABCC	ag-g+g+	δ
Nidippe_51.log:	158.9522	-57.3805	159.1802	-57.3362	-49.3116	ABAB	ag-ag-	δ
Nidippe_22.log:	158.4984	-57.5248	159.86	-57.6842	-49.3222	-		δ
Nidippe_100.log:	150.6677	76.7313	-104.63	-48.6184	-46.3551	ACBB	ag+g-g-	δ

Table 7, cont.

Nidippe_4.log:	150.2985	77.4052	-82.5334	-157.1532	-40.5389	ACBA	ag+g-a	δ
Nidippe_39.log:	149.3518	80.5851	56.3657	-160.5168	-40.6908	ACCA	ag+g+a	δ
Nidippe_16.log:	149.3489	80.4458	56.5066	-159.9034	-40.1827	-		δ
Nidippe_126.log:	152.0282	74.1725	54.7086	-19.41	-46.939	ACCB	ag+g+g-	δ
Nidippe_60.log:	151.0215	76.6403	159.2677	-57.5903	-45.8187	ACAB	ag+ag-	δ
Nidippe_5.log:	150.4791	77.8542	150.7429	77.8843	-41.9754	ACAC	ag+ag+	δ
Nidippe_28.log:	150.3385	78.1959	150.2835	78.4513	-41.9725	-		δ
Nidippe_33.log:	152.2201	77.3393	145.8621	176.699	-41.447	ACAA	ag+aa	δ
Nidippe_36.log:	152.6579	76.8957	146.0566	176.8355	-41.3263	-		δ
Nidippe_9.log:	152.6665	76.9821	145.909	176.9327	-41.2459	-		δ
Nidippe_25.log:	147.9721	176.0751	147.791	176.1401	-40.839	AAAA	aaaa	δ
Nidippe_70.log:	145.2469	177.1211	161.2415	-58.3359	-45.5167	AAAB	aaag-	δ
Nidippe_186.log:	145.2238	177.7052	55.5473	-19.7212	-47.3123	AACB	aag+g-	δ
Nidippe_187.log:	-177.8704	-145.107	19.9136	-55.5913	47.1248	AACB	aag+g-	λ
Nidippe_24.log:	-176.165	-147.508	-175.9762	-147.5982	41.1904	AAAA	aaaa	λ
Nidippe_113.log:	-120.668	80.7788	-176.7407	-146.5566	44.9933	ACAA	ag+aa	λ
Nidippe_55.log:	-120.593	81.9553	-77.2668	-151.4697	45.7169	ACBA	ag+g-a	λ
Nidippe_32.log:	-77.0325	-152.531	-177.0061	-145.7938	41.204	BAAA	g-aaa	λ
Nidippe_10.log:	-77.0693	-152.4602	-176.8429	-146.0256	41.2242	-		λ
Nidippe_37.log:	-152.6105	-76.7817	-176.8295	-145.9676	41.3948	-		λ
Nidippe_27.log:	-77.9211	-150.5137	-77.5903	-150.9353	41.9923	BABA	g-ag-a	λ
Nidippe_6.log:	-77.931	-150.5945	-77.4786	-150.928	41.9733	-		λ
Nidippe_59.log:	-76.728	-150.7428	57.5947	-160.2159	45.6725	BACA	g-ag+a	λ
Nidippe_125.log:	-73.9747	-152.4154	19.6928	-55.0178	46.687	BACB	g-ag+g-	λ
Nidippe_99.log:	-76.3063	-150.8043	48.0033	104.7712	46.267	BACC	g-ag+g+	λ
Nidippe_54.log:	-80.9394	-149.3054	159.7925	-56.3177	40.5726	BAAB	g+aag+	λ
Nidippe_17.log:	-78.1011	-150.7681	159.5162	-56.3141	40.023	-		λ
Nidippe_15.log:	-77.0192	-150.561	157.6784	82.6324	40.6142	BAAC	g+aag-	λ
Nidippe_3.log:	-76.444	-150.8314	158.2754	82.924	40.5846	-		λ
Nidippe_98.log:	-118.2606	-48.9141	-176.4673	-147.3449	44.9341	BBAA	g-g-aa	λ
Nidippe_72.log:	-118.228	-48.4062	-176.1196	-147.2482	45.3333	-	g-g-aa	λ
Nidippe_152.log:	-77.1133	-26.3209	-176.805	-145.9625	42.399	BBAA	g-g-aa	λ
Nidippe_104.log:	-77.1165	-26.4113	-176.858	-145.9586	42.3499	-	g-g-aa	λ
Nidippe_175.log:	-77.5683	-26.0756	-176.7771	-145.6226	42.6553	-	g-g-aa	λ
Nidippe_83.log:	-119.0421	-47.952	-76.9353	-151.9956	45.288	BBBA	g-g-g-a	λ
Nidippe_142.log:	-78.7729	-25.0519	-79.6874	-150.0595	43.2946	BBBA	g-g-g-a	λ
Nidippe_140.log:	-116.7767	-47.9027	-116.6832	-48.0688	49.9501	BBBB	g-g-g-g-	λ

Table 7, cont.

Nidippe_199.log:	-78.2207	-25.2704	-116.7475	-47.7955	46.8844	BBBB	g-g-g-g-	λ
Nidippe_233.log:	-81.4983	-24.7318	-74.6437	106.4762	44.2771	BBBC	g-g-g-g+	λ
Nidippe_122.log:	-115.5833	-48.2997	57.992	-158.5462	50.0502	BBCA	g-g-g+a	λ
Nidippe_66.log:	-115.9614	-48.6851	57.9111	-158.4701	49.8993	-		λ
Nidippe_159.log:	-79.3702	-25.1653	57.2696	-158.2687	46.8286	BBCA	g-g-g+a	λ
Nidippe_240.log:	-116.0342	-48.3162	19.5722	-54.0857	51.3566	BBCB	g-g-g+g-	λ
Nidippe_206.log:	-116.1951	-48.1096	19.421	-53.9145	51.3296	-		λ
Nidippe_173.log:	-116.6418	-48.3616	54.8787	-30.2916	49.4783	BBCB	g-g-g+g-	λ
Nidippe_165.log:	-116.3712	-48.5932	13.3361	82.535	50.9049	BBCC	g-g-g+g+	λ
Nidippe_229.log:	-81.9256	-24.8399	48.2218	105.5458	47.945	BBCC	g-g-g+g+	λ
Nidippe_176.log:	-116.5901	-48.1115	49.3477	105.6425	50.5795	BBCC	g-g-g+g+	λ
Nidippe_79.log:	-115.8782	-48.2971	160.4839	-55.8532	44.4922	BBAB	g-g-ag-	λ
Nidippe_116.log:	-85.4473	-24.4767	160.3271	-55.6773	42.3024	BBAB	g-g-ag-	λ
Nidippe_73.log:	-118.5671	-47.6371	157.3222	81.7789	44.3775	BBAC	g-g-ag+	λ
Nidippe_117.log:	-118.4723	-47.5453	157.8811	81.9234	44.4621	-		λ
Nidippe_53.log:	-118.933	-47.4558	157.9968	81.987	44.3704	-		λ
Nidippe_111.log:	-76.6955	-25.8066	157.3607	83.4497	41.8094	BBAC	g-g-ag+	λ
Nidippe_168.log:	-82.1428	-24.6795	160.0353	162.5241	43.6934	BBAA	g-g-aa	λ
Nidippe_143.log:	-74.9944	105.9226	-80.7838	-149.3659	43.4118	BCBA	g-g+g-a	λ
Nidippe_130.log:	-75.4052	106.0675	-176.7019	-146.0663	42.6738	BCAA	g-g+aa	λ
Nidippe_184.log:	-118.5281	81.2775	-116.0594	-47.9431	50.2158	BCBB	g-g+g-g-	λ
Nidippe_137.log:	-117.7615	80.7088	-118.6961	81.0552	50.5427	BCBC	g-g+g-g+	λ
Nidippe_213.log:	-75.7693	108.221	-118.3526	81.8917	47.7112	BCBC	g-g+g-g+	λ
Nidippe_180.log:	-78.406	107.36	-75.4698	106.4441	44.1731	BCBC	g-g+g-g+	λ
Nidippe_127.log:	-75.0202	106.44	57.0893	-158.8906	46.8984	BCCA	g-g+g+a	λ
Nidippe_102.log:	-117.2799	80.1556	57.8658	-158.5101	50.1114	BCCA	g-g+g+a	λ
Nidippe_166.log:	-117.4322	80.0989	58.0625	-158.3977	50.1689	-		λ
Nidippe_179.log:	-117.4649	80.879	19.6418	-54.3935	51.6539	BCCB	g-g+g+g-	λ
Nidippe_226.log:	-74.7787	107.3084	19.0829	-53.8548	48.5898	BCCB	g-g+g+g-	λ
Nidippe_211.log:	-74.6066	107.7344	18.9189	-53.5974	48.8071	-		λ
Nidippe_235.log:	-117.5653	80.873	54.2339	-30.1448	49.5479	BCCB	g-g+g+g-	λ
Nidippe_227.log:	-117.6516	80.8766	13.4756	81.8933	51.2797	BCCC	g-g+g+g+	λ
Nidippe_193.log:	-74.8529	107.2908	47.9356	105.7194	47.5247	BCCC	g-g+g+g+	λ
Nidippe_96.log:	-118.6455	81.4925	160.5575	-56.4253	44.5362	BCAB	g-g+ag-	λ
Nidippe_131.log:	-79.5688	107.4636	160.1035	-56.0193	41.881	BCAB	g-g+ag-	λ
Nidippe_85.log:	-74.734	107.4693	156.7293	83.354	42.1518	BCAC	g-g+ag+	λ
Nidippe_171.log:	-119.3751	81.7152	160.5128	161.9976	46.446	BCAA	g-g+aa	λ

Table 7, cont.

Nidippe_89.log:	-118.9555	81.7887	160.0181	162.9528	46.5875	-		λ
Nidippe_217.log:	58.1269	-158.4144	-116.1217	-48.3594	49.7071	CABB	g+ag-g-	λ
Nidippe_203.log:	57.9911	-158.0037	-115.8711	-48.4389	49.7526	-		λ
Nidippe_50.log:	57.3855	-158.7432	57.626	-159.3556	49.3248	CACA	g+ag+a	λ
Nidippe_23.log:	57.4035	-158.7715	57.6043	-159.32	49.3297	-		λ
Nidippe_191.log:	58.4522	-158.3925	19.9654	-54.8884	50.9232	CACB	g+ag+g-	λ
Nidippe_222.log:	57.605	-157.8065	54.2397	-30.2882	49.192	CACB	g+ag+g-	λ
Nidippe_78.log:	57.5549	-157.867	48.1839	105.2866	50.1585	CACC	g+ag+g+	λ
Nidippe_44.log:	57.3295	-158.8574	159.6597	164.1277	46.2028	CAAA	g+aaa	λ
Nidippe_135.log:	54.6237	-30.8334	-177.4198	-144.9093	45.3878	CBAA	g+g-aa	λ
Nidippe_88.log:	54.3378	-30.4599	-76.5098	-150.8707	45.1671	CBBA	g+g-g-a	λ
Nidippe_119.log:	54.275	-30.3445	-76.4515	-150.8611	45.2041	-		λ
Nidippe_242.log:	19.443	-53.8644	-116.2628	-48.4919	51.3121	CBBB	g+g-g-g-	λ
Nidippe_209.log:	19.5498	-53.7383	-116.3451	-48.3847	51.3895	-		λ
Nidippe_195.log:	53.9445	-29.8505	-74.3255	106.5001	46.5829	CBBC	g+g-g-g+	λ
Nidippe_200.log:	54.3085	-30.2339	54.2164	-30.4372	48.9437	CBCB	g+g-g+g-	λ
Nidippe_243.log:	54.2862	-30.2686	54.309	-30.2208	48.9763	-		λ
Nidippe_157.log:	19.5743	-54.6564	58.2212	-158.6545	51.1013	CBCA	g+g-g+a	λ
Nidippe_110.log:	19.3256	-54.4472	58.2608	-158.1511	50.855	-		λ
Nidippe_147.log:	19.6261	-54.0877	160.988	-55.5452	46.0448	CBAB	g+g-ag-	λ
Nidippe_145.log:	53.5798	-29.6507	159.9587	164.4166	45.9178	CBAA	g+g-aa	λ
Nidippe_34.log:	114.2039	118.7411	-163.0373	-162.6631	78.0367	CCAA	g+g+aa	λ
Nidippe_94.log:	13.2851	80.5378	-177.5206	-145.3859	46.4662	CCAA	g+g+aa	λ
Nidippe_123.log:	13.3816	79.7201	-177.3348	-145.2589	46.8075	-		λ
Nidippe_108.log:	12.9356	81.8229	-76.8296	-151.1984	46.562	CCBA	g+g+g-a	λ
Nidippe_163.log:	13.229	82.473	-116.0507	-48.2743	51.0844	CCBB	g+g+g-g-	λ
Nidippe_238.log:	49.0983	106.296	-116.0783	-47.9747	50.4924	CCBB	g+g+g-g-	λ
Nidippe_218.log:	13.0012	83.1625	-77.4573	-25.426	47.8518	CCBB	g+g+g-g-	λ
Nidippe_149.log:	13.6383	81.3381	57.6416	-158.0778	50.5863	CCCA	g+g+g+a	λ
Nidippe_223.log:	13.4974	82.1071	19.5693	-54.745	52.1094	CCCB	g+g+g+g-	λ
Nidippe_236.log:	49.7873	105.2178	19.0585	-54.2676	51.7561	CCCB	g+g+g+g-	λ
Nidippe_197.log:	13.1457	82.2737	54.0073	-30.3318	50.1977	CCCB	g+g+g+g-	λ
Nidippe_188.log:	13.1292	82.0466	13.2717	81.8456	51.8132	CCCC	g+g+g+g+	λ
Nidippe_160.log:	48.6134	105.6577	48.4358	105.7465	51.0944	CCCC	g+g+g+g+	λ
Nidippe_215.log:	48.2322	106.1766	48.1009	105.9689	51.05	-		λ
Nidippe_105.log:	13.4576	82.2233	160.5132	-56.0203	45.5405	CCAB	g+g+ag-	λ
Nidippe_151.log:	13.355	82.379	160.5306	-55.9865	45.5047	-		λ

Table 7, cont.

Nidippe_76.log:	47.4698	105.3485	157.4994	81.666	45.3438	CCAC	g+g+ag+	λ
Nidippe_46.log:	160.3939	-56.2806	57.2203	-158.9012	44.4787	ABCA	ag-g+a	λ
Nidippe_48.log:	160.7027	-56.9166	-177.0332	-145.5012	39.6143	ABAA	ag-aa	λ
Nidippe_30.log:	159.9744	-56.9083	-177.0565	-145.4155	39.6105	-		λ
Nidippe_64.log:	159.4884	-56.2928	159.6422	-56.2534	38.0221	ABAB	ag-ag-	λ
Nidippe_81.log:	160.2321	-55.984	156.6677	82.1201	38.6009	ABAC	ag-ag+	λ
Nidippe_43.log:	159.6401	-56.0424	157.1614	82.136	38.7003	-		λ
Nidippe_14.log:	159.6615	-56.0603	157.1823	82.1727	38.6971	-		λ
Nidippe_61.log:	159.4652	-55.6449	158.0239	163.0782	40.1465	ABAA	ag-aa	λ
Nidippe_18.log:	158.1067	81.252	56.2454	-159.2712	44.6739	ACCA	ag+g+a	λ
Nidippe_29.log:	158.2549	82.7156	-77.6068	-150.4133	40.5088	ACBA	ag+g-a	λ
Nidippe_8.log:	157.6814	80.8148	-177.1742	-145.185	40.1714	ACAA	ag+aa	λ
Nidippe_21.log:	158.2517	81.1198	-177.1307	-145.0313	40.2704	-		λ
Nidippe_26.log:	156.8996	82.1426	159.6475	-55.9974	38.6804	ACAB	ag+ag-	λ
Nidippe_41.log:	156.7181	82.259	160.5298	-55.952	38.4674	-		λ
Nidippe_11.log:	156.705	82.1528	160.4435	-55.9447	38.4674	-		λ
Nidippe_134.log:	157.8682	82.0874	13.0843	82.119	45.6277	ACCC	ag+g+g+	λ
Nidippe_2.log:	157.804	82.7177	157.8441	82.6726	39.5104	ACAC	ag+ag+	λ
Nidippe_68.log:	159.7938	163.3167	56.953	-158.4487	46.1531	AACA	aag+a	λ
Nidippe_154.log:	159.6566	164.0719	47.9604	105.7217	47.1811	AACC	aag+g+	λ
Nidippe_91.log:	157.9209	163.9282	157.7697	164.0476	42.0846	AAAA	aaaa	λ
Nidippe_57.log:	158.1512	164.0344	158.0806	164.1528	42.3305	-		λ

Table 8: Percent population calculations for optimized unique conformers.

k_B (kcal/molK)	T (K)	ΔG (kcal)	β (mol/kcal)	expt(-βΔG)	%
2.0E-03	298.2	0.0	1.7E+00	1.0E+00	1.6E+01
		0.1		8.4E-01	1.3E+01
		0.2		7.1E-01	1.1E+01
		0.3		6.0E-01	9.4E+00
		0.4		5.1E-01	7.9E+00
		0.5		4.3E-01	6.7E+00
		0.6		3.6E-01	5.6E+00
		0.7		3.1E-01	4.8E+00
		0.8		2.6E-01	4.0E+00
		0.9		2.2E-01	3.4E+00
		1.0		1.8E-01	2.9E+00
		1.1		1.6E-01	2.4E+00
		1.2		1.3E-01	2.0E+00
		1.3		1.1E-01	1.7E+00
		1.4		9.4E-02	1.5E+00
		1.5		8.0E-02	1.2E+00
		1.6		6.7E-02	1.0E+00
		1.7		5.7E-02	8.8E-01
		1.8		4.8E-02	7.4E-01
		1.9		4.0E-02	6.3E-01
		2.0		3.4E-02	5.3E-01
		2.1		2.9E-02	4.5E-01
		2.2		2.4E-02	3.8E-01
		2.3		2.1E-02	3.2E-01
		2.4		1.7E-02	2.7E-01
		2.5		1.5E-02	2.3E-01
		2.6		1.2E-02	1.9E-01
		2.7		1.0E-02	1.6E-01
		2.8		8.9E-03	1.4E-01
		2.9		7.5E-03	1.2E-01
		3.0		6.3E-03	9.8E-02
		3.1		5.3E-03	8.3E-02
		3.2		4.5E-03	7.0E-02
		3.3		3.8E-03	5.9E-02
		3.4		3.2E-03	5.0E-02
		3.5		2.7E-03	4.2E-02

Table 8, cont.

	3.6	2.3E-03	3.6E-02
	3.7	1.9E-03	3.0E-02
	3.8	1.6E-03	2.5E-02
	3.9	1.4E-03	2.2E-02
	4.0	1.2E-03	1.8E-02
	4.1	9.9E-04	1.5E-02
	4.2	8.3E-04	1.3E-02
	4.3	7.0E-04	1.1E-02
	4.4	6.0E-04	9.2E-03
	4.5	5.0E-04	7.8E-03
	4.6	4.2E-04	6.6E-03
	4.7	3.6E-04	5.6E-03
	4.8	3.0E-04	4.7E-03
	4.9	2.6E-04	4.0E-03
	5.0	2.2E-04	3.4E-03
	5.1	1.8E-04	2.8E-03
	5.2	1.5E-04	2.4E-03
	5.3	1.3E-04	2.0E-03
	5.4	1.1E-04	1.7E-03
	5.5	9.3E-05	1.4E-03
	5.6	7.9E-05	1.2E-03
	5.7	6.6E-05	1.0E-03
	5.8	5.6E-05	8.7E-04
	5.9	4.7E-05	7.4E-04
	6.0	4.0E-05	6.2E-04
	6.1	3.4E-05	5.2E-04
	6.2	2.9E-05	4.4E-04
	6.3	2.4E-05	3.7E-04
	6.4	2.0E-05	3.2E-04
	6.5	1.7E-05	2.7E-04
	6.6	1.5E-05	2.3E-04
	6.7	1.2E-05	1.9E-04
	6.8	1.0E-05	1.6E-04
	6.9	8.8E-06	1.4E-04
	7.0	7.4E-06	1.1E-04
	7.1	6.2E-06	9.7E-05
	7.2	5.3E-06	8.2E-05

Table 8, cont.

	7.3	4.5E-06	6.9E-05
	7.4	3.8E-06	5.8E-05
	7.5	3.2E-06	4.9E-05
	7.6	2.7E-06	4.2E-05
	7.7	2.3E-06	3.5E-05
	7.8	1.9E-06	3.0E-05
	7.9	1.6E-06	2.5E-05
	8.0	1.4E-06	2.1E-05
	8.1	1.2E-06	1.8E-05
	8.2	9.8E-07	1.5E-05
	8.3	8.2E-07	1.3E-05
	8.4	7.0E-07	1.1E-05
	8.5	5.9E-07	9.1E-06
	8.6	5.0E-07	7.7E-06
	8.7	4.2E-07	6.5E-06
	8.8	3.5E-07	5.5E-06
	8.9	3.0E-07	4.6E-06
	9.0	2.5E-07	3.9E-06
	9.1	2.1E-07	3.3E-06
	9.2	1.8E-07	2.8E-06
	9.3	1.5E-07	2.4E-06
	9.4	1.3E-07	2.0E-06
	9.5	1.1E-07	1.7E-06
	9.6	9.2E-08	1.4E-06
	9.7	7.8E-08	1.2E-06
	9.8	6.6E-08	1.0E-06
	9.9	5.5E-08	8.6E-07
	10.0	4.7E-08	7.3E-07
		$\sum ge^{-\beta\Delta G} =$ 6.4	

BIOGRAPHICAL SKETCH

Jennifer Sanchez was born and raised in McAllen, Texas, the south-pole of Texas, on the 24th of August 1998. Attended and graduated the International Baccalaureate program at Lamar Academy in 2016, while also attending James 'Nikki' Rowe High School for extracurricular activities, like Band and cross-country running. It was during this time where her interest in Chemistry flourished over playing the oboe or running. She then attended the University of Texas at Rio Grande Valley (UTRGV) where she graduated with a Bachelor of Science and Arts Degree in Chemistry and continued with pursuing her master's degree in chemistry. Jennifer worked as an Undergraduate Research Assistant for the Multifunctional Applications of Oxides (MAO) studying carbon dots, as a Peer-Lead-Team-Leader (PLTL) student academic tutor for Chemistry with the Learning center, and finally as a Graduate Teaching Assistant with the Chemistry department. Each one of these jobs solidifying her love for Chemistry and allowing her to expand her knowledge. Jennifer graduated with her M.S. Chemistry Degree from UTRGV on May 7th, 2022.

Current mailing address: 4524 W. Maple Ave. McAllen, Tx, 78501

Author can be reached at: Jensanch26@gmail.com